Cell Tissue Res (2001) 304:193–214
DOI 10.1007/s004410100363

REGULAR ARTICLE

R.E. Papka · M. Storey-Workley · P.J. Shughrue
I. Merchenthaler · J.J. Collins · S. Usip
P.T.K. Saunders · M. Shupnik

Estrogen receptor-α and -β immunoreactivity and mRNA in neurons of sensory and autonomic ganglia and spinal cord

Received: 16 October 2000 / Accepted: 22 January 2001 / Published online: 16 March 2001

Abstract Estrogen receptor-α immunoreactivity and mRNAs are present in neurons in locales that innervate genital organs, e.g., parasympathetic pelvic autonomic ganglia, sensory dorsal root and nodose ganglia, and autonomic areas of the lumbosacral spinal cord. With the availability of probes for the β-isoform of the estrogen receptor, we studied this receptor in autonomic, sensory, and spinal cord neurons and compared it with the distribution of the α-receptor. Estrogen receptor-α and -β immunoreactivity were located in the nuclei of neurons, were in subpopulations of parasympathetic neurons in pelvic ganglia, and sensory neurons of dorsal root and nodose ganglia. Both receptor subtypes were present in the lumbosacral spinal cord: in neurons of the outer laminae of the dorsal horn, lateral collateral and medial collateral pathways, sacral parasympathetic nucleus, dorsal intermediate gray, and lamina X. Similar numbers of spinal cord neurons were immunoreactive for estrogen receptor-β and estrogen receptor-α. However, estrogen receptor-β-immunoreactive neurons appeared less numerous in the outer dorsal horn, but more numerous in the deeper layers of the spinal cord than estrogen receptor-α neurons. Retrograde tracing from the uterus revealed "uterine-related" neurons in dorsal root and pelvic ganglia that contained estrogen receptor-α and -β. In situ hybridization revealed both estrogen receptor-α and -β mRNA transcripts in sensory neurons of the dorsal root and nodose ganglia, parasympathetic neurons of pelvic ganglia, and spinal cord neurons in the dorsal horn, sacral parasympathetic nucleus, and dorsal intermediate gray of L6-S1 segments. These studies show that both estrogen receptor-α and -β are synthesized by autonomic and sensory neurons in parts of the nervous system that have connections with the female reproductive system. Such neurons contain neurotransmitters that have important functions in the female reproductive organs; thus, it is likely that estrogen can influence the activity of such neurons and consequently, through them, the activities of the reproductive organs.

Keywords Pelvic ganglia · Dorsal root ganglia · Nodose ganglia · Capsaicin receptor · Vanilloid receptor · Calcitonin gene-related peptide · Rat (Sprague Dawley)

This work was supported in part by NIH grants NS22526 and NS33081

R.E. Papka (✉) · M. Storey-Workley · J.J. Collins · S. Usip
Department of Neurobiology and Pharmacology,
Northeastern Ohio Universities College of Medicine,
PO Box 95, 4209 State Rt. 44, Rootstown, OH 44272, USA
e-mail: rpapka@neoucom.edu
Tel.: +1-330-3256636, Fax: +1-330-3255916

P.J. Shughrue · I. Merchenthaler
Women's Health Research Institute, Wyeth-Ayerst Research,
Radnor, Pa., USA

P.T.K. Saunders
MRC Reproductive Unit, Center for Reproductive Biology,
Edinburgh, UK

M. Shupnik
Department of Medicine,
University of Virginia Health Sciences Center,
Charlottesville, Va., USA

Introduction

The genomic effects of estrogens are mediated by nuclear estrogen receptors (ER) that, when bound to their ligand, undergo conformational changes and bind to chromatin to modulate transcription of target genes (Murdoch and Gorski 1991). Until recently, the ER was thought to exist as a single isoform, the classic ER-α. However, recent cloning experiments have identified another isoform of the ER, which is designated ER-β (Kuiper et al. 1996; Mosselman et al. 1996; Tremblay et al. 1997). There is marked conservation of amino acid sequences between the two forms in the DNA-binding domain and moderate conservation in the ligand (hormone)-binding domain (Mosselman et al. 1996; Kuiper et al. 1997;Tremblay et al. 1997; Couse and Korach 1998). Both receptors have similar affinities for binding estradiol (Mosselman et al. 1996; Kuiper et al. 1997). However, the tissue distribu-

tion and level of expression of ER-α and ER-β varies in prostate, ovary, uterus (Kuiper et al. 1996, 1997, 1998; Mosselman et al. 1996; Couse and Korach 1998; Shughrue et al. 1998a; Hiroi et al. 1999), and various parts of the brain (Shughrue et al. 1997). In addition, there are significant amino acid differences in the regions of these receptors that would be expected to influence transcriptional activity (Hall and McDonnell 1999). These data suggest that there might be different roles for ER-α and ER-β in estrogen-responsive tissues. Furthermore, certain compounds such as tamoxifen citrate and the phytoestrogens have differential actions that are tissue specific and the different ER subtypes may help explain these effects (Paech et al. 1997; Kuiper et al. 1999).

Within the nervous system, estrogen reportedly has an array of effects on many different neuronal systems. These include stimulating the outgrowth and development of neurite processes (Toran-Allerand 1976; Thorbert et al. 1978), acting as a growth factor (Matsumoto et al. 1988; Honjo et al. 1992), regulation of sensory neuronal survival (Patrone et al. 1999), stimulating synaptic plasticity (Langub et al. 1994; McEwen et al. 1991; McEwen 1996), and inducing and accelerating neurotransmitter expression (Okamura et al. 1994a, 1994b; McEwen 1996). These effects largely occur in neurons that have demonstrable ERs. The relative contributions of ER-α and ER-β to producing these effects are not well understood. A differential expression of ER-α and ER-β mRNAs has been described in the brain (Shughrue et al. 1997) and more recently in the dorsal root ganglia (DRG; Taleghany et al. 1999). Previous studies have shown the existence of radiolabeled estradiol binding (Keefer et al. 1973; Morrell et al. 1982) and ER-α immunoreactivity (Amandusson et al. 1996; Williams and Papka 1996) in spinal cord neurons, and ER-α immunoreactivity in autonomic and sensory ganglionic neurons (Papka et al. 1997; Yang et al. 1998; Taleghany et al. 1999). Furthermore, a study by Taleghany et al. (1999) has reported a comparison of ER-α and -β mRNAs in DRG, but to date studies have not examined ER-β immunoreactivity in autonomic parasympathetic or sensory nodose ganglia (NG). Moreover, though ER-β has been detected by reverse transcriptase polymerase chain reaction (Kuiper et al. 1997) and by in situ hybridization histochemistry (Shughrue et al. 1997), detailed examination of the distribution of ER-β immunoreactivity or ER-β mRNA expression in autonomic ganglia or spinal cord, especially in relation to ER-α, has not been reported. Thus, the goals of the present study were to (1) determine whether the ER-β protein is present in autonomic and sensory ganglionic neurons and spinal cord neurons, and (2) compare the presence and distribution of ER-α and ER-β in ganglionic and spinal cord neurons by using immunohistochemistry and in situ hybridization histochemistry. The results of this study suggest that estrogen could influence structural and functional (activity/neurochemistry) parameters of autonomic and sensory ganglionic neurons and spinal cord neurons in areas concerned with innervation of female reproductive organs.

Materials and methods

Animals

Adult female Sprague-Dawley rats (180–250 g body weight; SASCO strain from Charles Rivers) were used in this study. All experiments were performed in accordance with the NIH *Guide for the Care and Use of Laboratory Animals* (NIH Publications No. 86-23, revised 1985). During all experiments, efforts were made to minimize both animal suffering and numbers of animals used.

General methods

Ovariectomy

Twenty-four rats (13 ovariectomized and 11 intact) were used in this study. The stage of the estrous cycle was not determined in the intact rats. For ovariectomy, animals were anesthetized with sodium pentobarbital (45 mg/kg i.p.) and ovaries removed via two small dorsal incisions. Incisions were closed with a single stitch to the muscle layer and a single wound-clip to the skin. After 7–10 days survival the rats were perfused with fixative and tissues harvested.

Perfusions

Rats, intact and ovariectomized, were deeply anesthetized (100 mg/kg sodium pentobarbital i.p.) and exsanguinated by cardiac perfusion with saline followed by 4% paraformaldehyde in 0.1 M phosphate buffer, pH 7.3. The L6-S1 segments of the lumbosacral spinal cords were removed, cryoprotected in 30% sucrose, frozen, and sectioned (40 µm thick) coronally on a cryostat. In addition, the L6-S1 DRG, pelvic paracervical parasympathetic ganglia (PG), vagal NG, and the uterine cervix were removed, cryoprotected, and sectioned (14 µm thick). Sections were then processed for immunohistochemistry and stained for ER-α or ER-β.

Immunohistochemistry

Immunostaining for ER immunoreactivity, calcitonin gene-related peptide (CGRP) immunoreactivity, and vanilloid receptor subtype 1 (VR1; capsaicin receptor) was performed by standard techniques routinely used in our laboratory (Williams and Papka 1996; Papka et al. 1997; Collins et al. 1999, 2000). The sections of spinal cord, PG, DRG, and NG were incubated with primary antisera (see Table 1): rabbit-generated anti-ER-α antiserum, sheep-generated anti-ER-β antiserum, rabbit-generated anti-CGRP, and guinea pig-generated anti-VR1, for 16–24 h at room temperature. They were then washed in phosphate-buffered saline (PBS), incubated in appropriate secondary antibodies (see Table 1): CY-2 or CY-3-labeled goat anti-rabbit IgG; Texas Red-conjugated goat anti-guinea pig; and Alexa 488-labeled goat anti-rabbit IgG or Alexa 488-labeled donkey anti-sheep IgG, for 1 h, and mounted in PBS-glycerol. Some tissues were incubated with biotinylated anti-sheep IgG and visualized with Texas Red conjugated to avidin, while others were incubated with biotinylated goat anti-rabbit IgG (diluted 1:600) for 2 h in the primary antisera and then ER immunoreactivity visualized using the Vector diaminobenzidine (DAB), Vector SG, or Vector VIP peroxidase substrate kits. The peroxidase-treated sections were dehydrated through graded alcohol dilutions to toluene and then mounted on slides with Permount.

Tissue sections were viewed with an Olympus Provis microscope equipped for epifluorescence [single excitation and emission filters for Alexa488/fluorescein isothiocyanate (FITC)/CY-2 and tetramethyl rhodamine isothiocyanate (TRITC)/Texas Red/CY-3], brightfield, and darkfield microscopy. Images were captured with a Spot digital camera (Diagnostics Instruments, Sterling Heights, Mich.). Digitized images were imported into Photoshop version

Table 1 Antisera used in immunohistochemistry (*1°* first layer, *2°* second layer)

	Host	Dilution	Source
1° Antisera (Code)			
ER-α (C1355)	Rabbit	1:100	Dr. Margaret Shupnik, University of Virginia, Charlottesville, Va.
ER-β (893/3/34; 41/P3)	Sheep	1:5000	Dr. Phillipa Saunders, MRC, Edinburgh, UK
ER-β (Suffolk)	Sheep	1:5000	Dr. Istvan Merchanthaler, Women's Health Research Inst., Wyeth-Ayerst Research, Radnor, Pa.
CGRP	Rabbit	1:1600	Peninsula Laboratories, Belmont, Calif.
VR1(VR1C)	Guinea pig	1:400	Dr. Robert Elde, University of Minnesota, Minneapolis, Minn.
2° Antibody			
Anti-sheep, Biotinylated Texas Red avidin D	Rabbit	1:600	Vector Laboratories, Burlingame, Calif.
Anti-rabbit, CY-2	Goat	1:600	Jackson ImmunoResearch Labs, West Grove, Pa.
Anti-rabbit, CY-3	Goat	1:600	Jackson ImmunoResearch Labs, West Grove, Pa.
Anti-rabbit, Alexa 488	Goat	1:600	Molecular Probes, Eugene, Ore.
Anti-sheep, Alexa 488	Donkey	1:600	Molecular Probes, Eugene, Ore.
Anti-guinea pig, Texas Red	Goat	1:400	Jackson ImmunoResearch Labs, West Grove, Pa.

5.0 (Adobe Systems, San Jose, Calif.), contrast and brightness adjusted if necessary, labeled, and then printed with a Codonics 1,600 dye-sublimation printer (for color) or a 5750 Xerox Office 6 Copier (for black and white).

Populations of ER-positive cells

Tissue sections from ganglia (PG, NG, and DRG) and spinal cords were immunostained for ER-α or ER-β and neurons estimated in order to present an idea of relative frequency (in terms of percentage) of a subpopulation of ER-positive neurons within a general population of ganglion cells. Our criteria for counting cells included making an assumption that a section through a neuron with a distinct ER-labeled nucleus was a profile to be counted as labeled, and that a section through a neuron with an unlabeled nucleus (visible black hole in the cell cytoplasm under fluorescence microscopy) was a profile to be counted as unlabeled. Neurons in which neither a distinctly labeled nor unlabeled nucleus could be identified, i.e., a profile sectioned through cytoplasm, were omitted from both populations and not counted. Thus, all cells counted had to have been sectioned through the nucleus (using the assumption that a section through the nucleus was at or near the center of the cell). Also within our criteria was that only nonadjacent sections would be examined to ensure that we would avoid double-counting neurons. Twenty randomly chosen fields from two sections mounted on a slide from each ganglia of each animal were photographed with a digital Spot camera using a ×20 objective and printed. From the prints, the number of ER-positive cells (α or β) and number of ER-negative cells were estimated and the mean ± SEM was calculated using GB-StatJ v5.0 (Dynamic Microsystems), and the percentage of ER-positive neurons in each type of ganglion was calculated. Blocks of spinal cord containing the L6-S1 segments were serially sectioned (40-μm-thick sections) and about 60–65 sections per block were collected and placed in vials containing 0.01 M PBS. Ten free-floating sections were selected at random from the vials and immunostained for ER-α and ten for ER-β immunoreactivity. The sections were mounted on slides and ER-immunoreactive nuclear profiles mapped and counted per section using the assumption (Abercrombie 1946) that an immunostained nucleus represents a neuron. Only the dorsal one-half of the spinal cord sections were studied. Cells were counted in three regions designated as dorsal horn (DH), lateral collateral pathway + sacral parasympathetic nucleus (SPN/LCP), and dorsal intermediate gray (DIG) and the number of ER-positive neurons determined for each area. The number of ER-positive neurons was expressed as mean per spinal cord section (it was not feasible to accurately identify and count all projection neurons, interneurons, etc. that were ER-negative in the cord, thus percentages were not calculated).

Characterization of antisera

The studies of ER-α immunoreactivity were carried out primarily with the antiserum coded C1355 (Friend et al. 1997), though antisera from other sources were used for comparisons and they produced similar localization patterns to C1355 in respective nerve tissues. Other antisera against ER-α used in previous studies include an antiserum made in rat against the human ER code H222 (Li et al. 1993; Williams and Papka 1996; obtained from Abbott Laboratories, North Chicago, Ill.), rabbit anti-ER code AS409 (Okamura et al. 1992; Papka et al. 1997), rabbit anti-ER code NIH715 (Furlow et al. 1990; obtained from Dr. A.F. Parlow at the National Hormone and Pituitary Program, UCLA, Calif.), and mouse monoclonal anti-human ER antiserum code 1D5 (Collins et al. 1999; Dako, Glostrup, Denmark). In our hands, the C1355 produced the most consistent robust signal with immunofluorescence; thus this antiserum for ER-α was used for these studies.

The ER-α antiserum C1355 was raised against the last 14 amino acids of the ER (Friend et al. 1997). The ER-β antisera were raised in sheep against the N-terminal (code 893/3/34 and 41/P3) and the hinge (code 913/l/36/P4) regions of the ER protein (Saunders et al. 2000) or against the last 21 amino acids of the rat ER-β protein (code Suffolk). Controls included omission of the primary antiserum, omission of the secondary antibody, absorption of the primary antiserum with its respective antigen (10 μg/ml of diluted antiserum), and cross-absorption controls. For the latter, the ER-α antiserum was absorbed with the ER-β peptide and then applied to tissue sections – the ER-α immunostaining appeared normal. Likewise, adsorbing ER-β antiserum with ER-α protein did not diminish immunostaining for the ER-β.

The CGRP antiserum has been used extensively in our laboratory and its characterization reported previously (Shew et al. 1991; Papka and McNeill 1992b, 1993). The VR1 antiserum was generated in a guinea pig against the C-terminal residues 816–838 of VR1, purified and characterized by Guo et al. (1999)

Retrograde tracing with fluorogold

To determine whether ER-containing sensory and autonomic ganglionic neurons and/or VR1-immunoreactive neurons projected axons to the uterus and uterine cervix, rats (*n*=3) were injected with the retrograde tracer fluorogold (FG). Prior to all surgical procedures, rats were anesthetized with sodium pentobarbital (45 mg/kg i.p.) or a mixture of ketamine and xylazine (86 mg/kg and 13 mg/kg, respectively, i.p.). A laparatomy was performed and approximately 2 μl of a 4% solution of FG in lactated Ringer's solution (Fluorochrome, Englewood, Colo.) was injected at multiple sites in the uterine cervix and lower one-third of the uterine horns.

After completion of the injections, the sites were sealed with New Skin (Medtech Labs, Cody, Wyo.), and a "membrane" made from parafilm was placed between the uterus and urinary bladder to insure that FG did not contact the bladder. After a 14-day survival period to allow for transport of the tracer, the L6-S1 DRG, PG, and NG were removed. The tissues were fixed and processed as described previously. Cryostat sections containing FG-labeled cells were processed for visualization of ER or VR1 by immunohistochemistry.

In situ hybridization

Probes. In situ hybridization for ER-α and ER-β mRNAs were done using very specific riboprobes for each of the ER receptors. The probe for ER-α (coded ERα-800; Shughrue et al. 1997) contained an 803-bp fragment of the original rat ER-α cDNA sequence (Koike et al. 1987). The probe for ER-β was a cocktail (ERβ 285/558) of two cRNA probes (fragment ERβ-558, bases 52–610; and fragment ERβ-285, bases 1809–2094; Shughrue et al. 1996a). Plasmids were linearized and used to generate [^{35}S]UTP-labeled cRNA probes for in situ hybridization.

In situ hybridization

Tissue processing. Intact and ovariectomized rats were anesthetized and perfused with saline as described previously. Tissues (PG, L6-S1 DRG, NG, L6-S1 spinal cord segments, and uterine cervix) were rapidly removed, frozen, sectioned on a cryostat, mounted on slides and stored desiccated at –86°C until processed for in situ hybridization. Prior to processing, sections were allowed to warm slowly by temporary storage in a –20°C freezer (1 h), at 4°C (1 h) and then at ambient temperature (1 h) before being exposed to air. The in situ hybridization protocol used has been described in detail by Shughrue et al. (1996b). Briefly, tissue sections were fixed for a short time in 4% paraformaldehyde in 0.01 M phosphate buffer, treated with acetic anhydride, delipidated, and dehydrated. Slide-mounted sections were hybridized with 200 µl of an antisense riboprobe (ER-β-285/558 or ER-α-800; 6×10^6 DPM/probe/slide) and 50% formamide hybridization mix. The sections were placed in a sealed, humidified chamber and incubated overnight at 55°C. The following day, the sections were immersed in 2 × SSC (0.3 M NaCl, 0.03 M sodium citrate; pH 7.0)/10 mM DTT, treated with RNase A (20 µg/ml), and washed (twice for 30 min at 65°C) in 0.l × SSC to remove nonspecific label. The slides were then dipped in NTB2 nuclear emulsion (Kodak; diluted 1:1 with distilled water) and exposed for 30–60 days in light-tight black desiccating boxes. After exposure, the sections were photographically processed, stained lightly with cresyl violet, and coverslipped. The slides from all animals were hybridized, washed, exposed, and photographically processed together to eliminate differences due to interassay variation in conditions. The sections were examined with brightfield and darkfield microscopy to detect the presence of reduced silver grains over perikarya of ganglionic and spinal cord neurons and epithelial and stromal cells of the uterine cervix.

Neurons were considered labeled if the number of silver grains over a neuron was 3 times greater than the number of grains over an equivalent area of (1) nonneural tissue, (2) neural tissue that was not the cell body, or (3) emulsion. The neural tissue other than the cell body and the nonneural tissue used for comparisons were nerve trunks entering or passing through ganglia, ganglionic connective tissue capsules, white matter of the spinal cord, or ependymal cells around the central canal. These tissues and emulsion would be expected to show minimal background levels of labeling. Thus background, i.e., the grains in the emulsion or over the nonneuronal tissue, was set at 1.0, and then the density of grains over the neurons had to be at least 3 times background for the neuron to be counted as ER-α mRNA-positive or ER-β mRNA-positive. The numbers of ER-α mRNA-expressing neurons or ER-β mRNA-expressing neurons in the spinal cord were estimated as described for the ER-immunoreactive neurons.

Results

Previous reports have outlined the presence and distribution of ER-α immunoreactivity in autonomic and sensory ganglia (Papka et al. 1997; Collins et al. 1999) and in lumbosacral spinal cord (Amandusson et al. 1995; Williams and Papka 1996), thus only highlights and additional details will be reported here so that comparisons with ER-β can be meaningful.

ER-α immunoreactivity in ganglia

ER-α protein was present in the nuclei of a subpopulation of parasympathetic neurons in the PG (Fig. 1A, B) and sensory neurons in the L6-S1 dorsal root (DRG; Fig. 1C, D) and vagal NG (Fig. 1E, F). Of the neurons in various ganglia, about 5.5% were ER-α-immunoreactive in the PG, 2.8% in the NG, and 5.3% were ER-α-immunoreactive in the DRG (Table 2). Neurons of sensory ganglia are in three size categories: large (more than 41 µm diameter), medium (21–40 µm diameter), and small (less than 20 µm; sizes based on studies (Rambourg et al. 1983; Price 1985; Tuchscherer and Seybold 1985; Papka and McNeill 1992a). ER-α-immunoreactive sensory neurons were predominantly in the small- but also medium-size categories (Fig. 1C, D). Furthermore, immunostaining with an antiserum against the capsaicin receptor (VR1; Caterina et al. 1997; Guo et al. 1999) was performed to "mark" mainly small, capsaicin-sensitive, polymodal nociceptive neurons (and some Aδ-neurons). VR1-immunoreactive + ER-α-immunoreactive neurons

Fig. 1A–G Sections of the pelvic ganglion (PG), dorsal root ganglia (DRG), and nodose ganglia (NG) of an ovariectomized rat immunostained for estrogen receptor-α (ER-α). **A** Low-magnification view of the PG. The nuclei (*arrows*) of some PG neurons are immunoreactive for ER-α. **B** Higher-magnification view of the PG showing several ER-α-positive PG neurons (*arrows*). **C** Low-magnification view of a section of a DRG showing scattered neurons immunoreactive for ER-α. Some immunoreactive neurons appear to be medium (*M*) and small (*S*) in size. Many of the large (*L*) neurons are not labeled. *Inset*: Higher-magnification view of a small- (*S*) and a medium (*M*)-sized ER-α-immunoreactive neuron in the DRG. Little cytoplasm is evident around the small neurons, which makes them difficult to identify. **D** A medium-magnification view of large (*L*), medium (*M*), and small (*S*) DRG neurons. In this field only the small neurons are ER-α-immunoreactive. **E** NG shows several neurons immunoreactive for ER-α (*arrows*). One neuron (*lower right arrow*) is cut tangentially through the nucleus so that that nuclear boundary does not appear sharp. **F** Higher-magnification view of the NG showing ER-α-immunoreactive neurons (*arrows*). **G** Section of DRG double-immunostained for vanilloid receptor subtype 1 (VR1) (*red cytoplasm*) and ER-α (*green nucleus*). Note several small neurons double-stained, while larger neurons (*L*) are negative for both ER-α and VR1. *Inset*: Same tissue as in **G**, which illustrates that some neurons in the DRG were VR1-positive but not ER-α-positive (neuron on the *left* with *red cytoplasm* surrounding an unstained ER-α-negative nucleus). Some neurons were ER-α-positive but VR1-negative (neuron on the *right* with a *green nucleus* surrounded by unstained cytoplasm). *Bar* 10 µm

were evident throughout the DRG, and most of the double-labeled neurons were small (Fig. 1G). We have previously reported that some ER-α-immunoreactive ganglionic neurons project axons to the uterus or uterine cervix (Papka et al. 1997).

ER-β immunoreactivity in ganglia

ER-β immunoreactivity was present in a subpopulation of neurons in the PG (Fig. 2A). Such neurons appeared to be randomly distributed in the ganglion without any

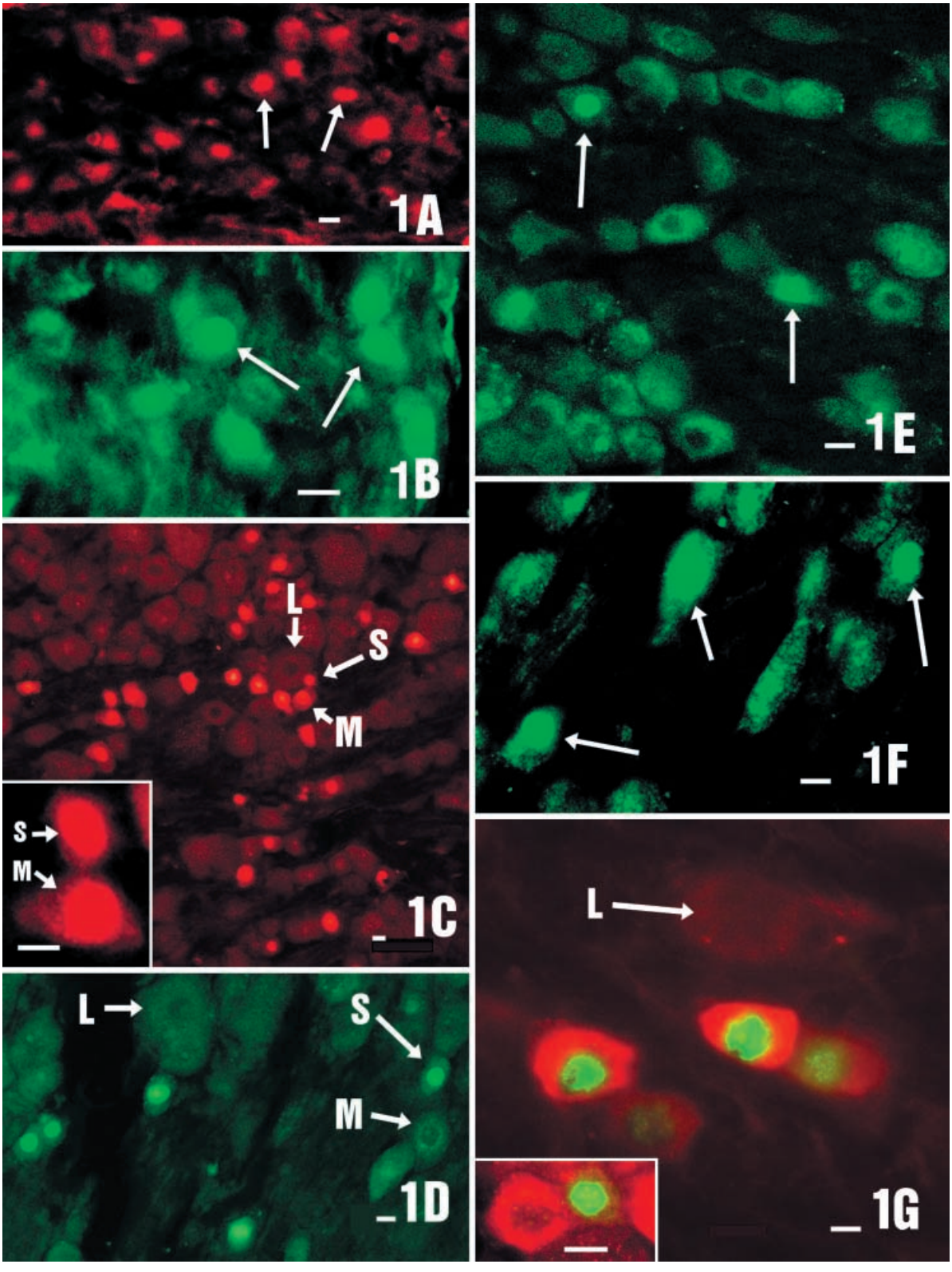

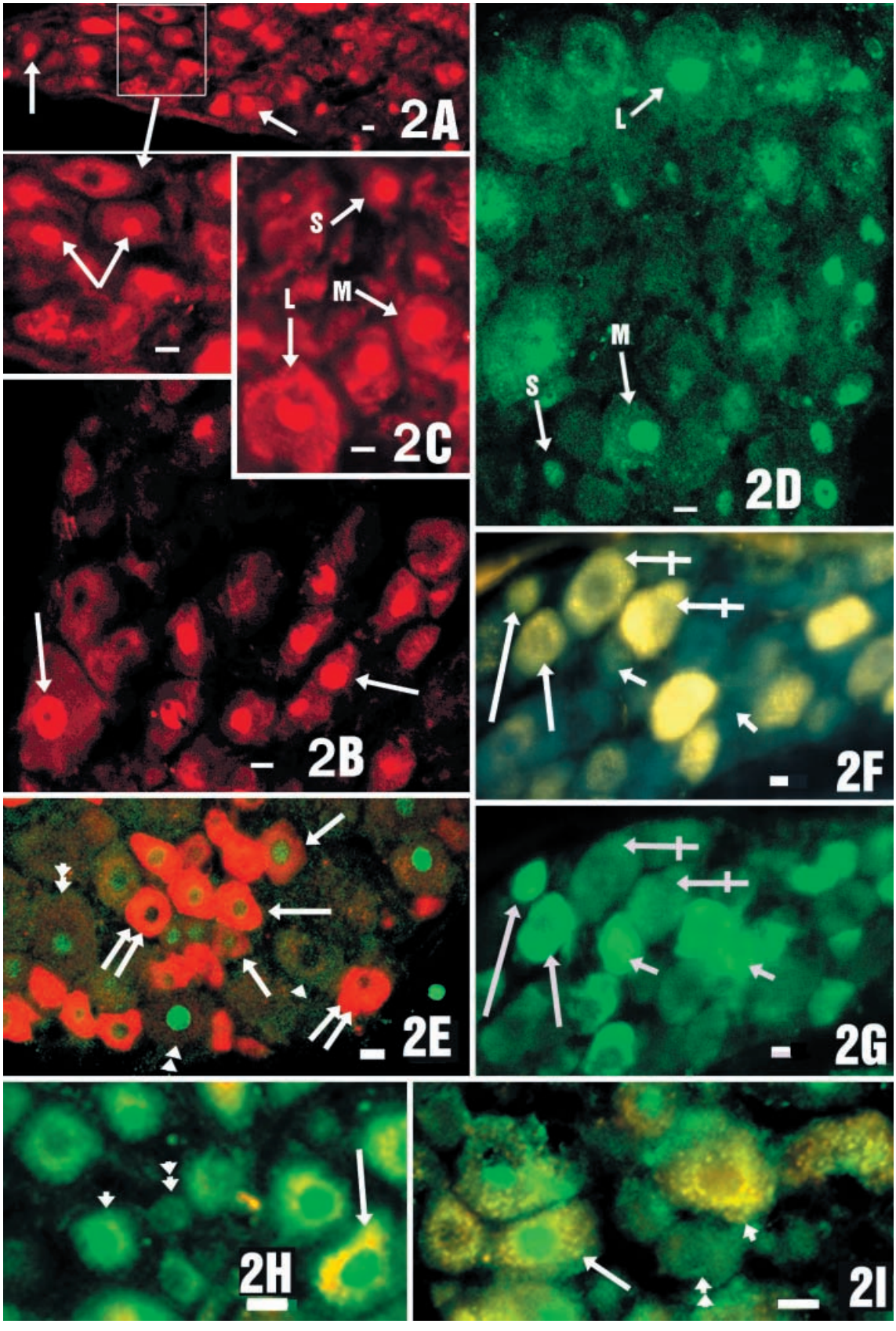
2A
2C
S
L
M
2D
L
M
S
2B
2F
2E
2G
2H
2I

Table 2 Mean numbers of estrogen-receptor (ER)-immunoreactive neurons counted in ganglia from ovariectomized rats and the percentage of cells that are ER-immunoreactive in those ganglia (*PG* pelvic ganglion, *DRG* dorsal root ganglia, *NG* nodose ganglia)

Ganglia	ER(+) cells (mean ± SEM)		ER(-) cells (mean ± SEM)		Total cells counted[a]		ER(+) ganglion cells (%)	
	ER-α	ER-β	ER-α	ER-β	ER-α	ER-β	ER-α	ER-β
PG	67.0±9.2	133.3±20.2	1143.3±207.8	1213.3±123.6	3631	4034	5.5	9.8
DRG	143.3±47.5[b]	78.3±8.2	2539.3±91.9	2012.3±93.4	8048	6273	5.3	3.8
NG	56.3±4.4	77.3±18.2	1983.0±241.5	2329.0±392.6	6118	7219	2.8	3.2

[a] Neurons counted in three rats

[b] There is noted variability in the numbers of ER-α-immunoreactive neurons in DRG, because the L6 and S1 ganglia were pooled for sectioning and counting. In fact, there are differential numbers of ER-positive neurons in L6 versus S1 ganglia, and we note that about 8.3% of neurons in the L6 DRG are ER-positive compared with approx. 4.2% in the S1 ganglia

apparent localization pattern. ER-β-immunoreactive neurons were more numerous in the PG than ER-α-immunoreactive neurons (9.8% vs 5.5%; see Table 2). In the L6-S1 DRG and vagal NG, ER-β-immunoreactive neurons appeared to be randomly scattered, although occasionally small, loosely aggregated clusters were evident (Fig. 2B, C, D). ER-β-immunoreactive sensory neurons appeared to be of all sizes, though most were medium- and small-sized (Fig. 2B, C, D). Of the neurons in various ganglia, 9.8% were ER-β-immunoreactive in the PG, 3.2% in the NG, and 3.8% in the DRG (Table 2). Immunostaining with the antiserum against the capsaicin receptor (VR1) marked capsaicin-sensitive, sensory neurons that were also ER-β-immunoreactive (Fig. 2E). After injecting the retrograde tracer FG into the uterus and uterine cervix, labeled neurons were evident in the PG, L6-S1 DRG, and NG. Some of these uterine-related (FG-containing) neurons also were VR1 immunoreactive (Fig. 2F, G) and ER-β immunoreactive (Fig. 2H, I).

◀ **Fig. 2A–I** Sections of the pelvic ganglion (PG), dorsal root ganglia (DRG) and nodose ganglia (NG) of an ovariectomized rat immunostained for ER-β. **A** The nuclei (*arrow*) of some PG neurons are immunostained for ER-β. However, the numbers of such neurons can vary in different fields. *Inset*: Higher-magnification view of the *boxed area* of Fig. 2A shows ER-β-immunoreactive PG neurons. The nuclei are the sites of ER-β immunoreactivity and they are surrounded by ER-β-negative cytoplasm. **B** Section of a DRG showing large and medium neurons that have ER-β-immunoreactive nuclei. **C** Shows a higher magnification view of large (*L*), medium (*M*), and small (*S*) DRG neurons that are ER-β-immunoreactive. **D** NG shows small (*S*), medium (*M*), and large (*L*)-sized ER-β-immunoreactive neurons. **E** Section of DRG immunostained for VR1 (*red cytoplasm*) and ER-β (*green nucleus*). Note several neurons are negative for both VR1 and ER-β (*arrowhead*), some large neurons are only ER-β-positive (*double arrowhead*), some medium-sized neurons are only VR1-positive (*double arrow*), some medium and small neurons are double-stained for both ER-β and VR1(*arrow*). **F, G** Section of DRG from a rat injected with fluorogold (FG; **F**) into the uterus and immunostained for VR1 (*green cytoplasm* in **G**). Neurons containing FG (*long arrows* in **F**) are considered "uterine-related" and some of them are VR1-immunoreactive (*long arrows* in **G**). Some neurons contain VR1 immunoreactivity, but not FG (*short arrows* in **E, F**), and some contain FG without VR1 immunoreactivity (*crossed arrows* in **F, G**). **H** PG from a rat injected with fluorogold into the uterus. A FG-positive, uterine-related neuron is ER-β-immunoreactive (*arrow*); other neurons in the field are ER-β-positive but do not contain the tracer (*arrowhead*), and still others are neither FG- nor ER-β-positive (*double arrowhead*). **I** DRG from a rat injected with FG into the uterus. A FG-positive, uterine-related neuron is ER-β-immunoreactive (*arrow*); other neurons in the field are FG-positive but do not contain ER-β (*arrowhead*), and still others are neither FG-positive nor ER-β-positive (*double arrowhead*). *Bar* 10 μm

ER-α mRNA-expressing neurons in ganglia

Autoradiograms revealed lightly, moderately, and densely labeled postganglionic parasympathetic neurons of the PG that expressed ER-α mRNA (Fig. 3A, B). With our paradigm, most labeling was regarded to be light to moderate. The ganglion sections (PG, DRG, and NG) were counterstained lightly with cresyl violet, which highlights the nucleus for cell identification but leaves the perikarya nonevident. However, staining the cytoplasm can interfere with the ease of reading the labeling (but helps in making cell-diameter measurements). Thus, we focused on silver grains associated with the nuclei of neurons and assumed that grains immediately adjacent to the nuclei were in the cytoplasm of the neurons (in some cases we did stain the cytoplasm to identify the entire perikaryon; e.g., see Fig. 3C, D).

The ER-α mRNA-expressing neurons, though only estimated, appeared to correspond in number per ganglion to those showing ER-α protein by immunohistochemistry (see Figs. 1A, B and 3B, C). Ganglionic neurons from ovariectomized rats appeared to be more heavily labeled for ER-α-mRNA expression than those from intact rats (Fig. 3A, B). However, we did not discern whether there were differences in numbers of labeled neurons between intact and ovariectomized rats. Satellite and Schwann cells were not labeled in the autoradiograms of the PG (Fig. 3) or sensory ganglia (Fig. 4). Moreover, areas of nerve trunks rich in axons, but neuron-free, did not show any labeling above background level.

Sensory neurons of the DRG and NG also expressed ER-α-mRNA that varied from light, to moderate, to dense labeling (Fig. 4A–F). For the most part, neurons with the densest labeling were small neurons (Fig. 4B),

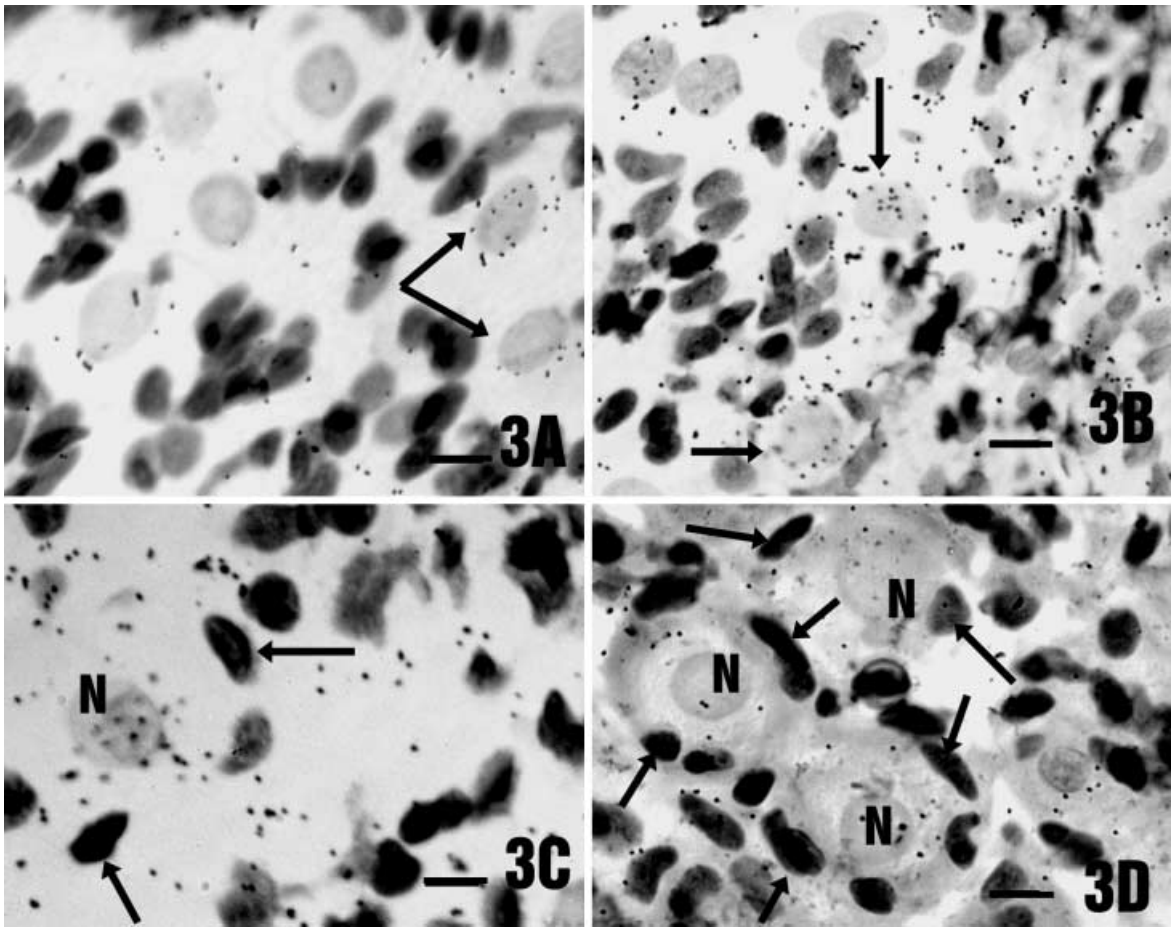

Fig. 3A–D ER-α mRNA in the female rat PG by in situ hybridization. **A**, **C,** and **D** are from an intact rat, whereas **B** is from an ovariectomized rat. In **A** neurons (*arrows*) are lightly labeled with silver grains for ER-α mRNA, whereas in **B** some neurons (*arrows*) are distinctly labeled with overlaying silver grains, indicating the presence of ER-α mRNA. **C** represents a section lightly counterstained with cresyl violet indicative of the routine counterstain for autoradiographic sections. With this stain the cytoplasmic extent of the neurons (*N*) is not readily evident, making the tissue appear "empty." The presence of satellite cells (*arrows*) helps to delimit the extent of the perikaryon. Thus, it is possible that some nonnuclear silver grains could be misinterpreted as not representing specific label. **D** is a section similar to **C** but counterstained with hematoxylin and eosin, which more fully stains the neurons (*N*) and satellite cells (*arrows*) and indicates that neuronal cytoplasm fills all of the "apparent empty" spaces in nerve tissue. Thus, one can be assured that silver grains in "spaces" surrounding neurons in the PG, as well as DRG and NG, actually are overlying neuronal cytoplasm. *Bar* 10 μm

some medium-size neurons were moderately labeled (Fig. 4C), and occasionally large neurons were lightly positive. In DRG, there were approximately six to ten small ER-α mRNA-expressing neurons per ganglion section and three or four lightly labeled, medium-size neurons. However, not all small neurons in the ganglia expressed ER-α mRNA.

In the NG, fewer neurons per section (four to six total neurons with two or three being small) expressed ER-α mRNA than in DRG. In all sensory ganglia it appeared that autoradiograms showed more labeling for ER-α mRNA in the ovariectomized rats than in the intact rats (Fig. 4E–F); however, whether or not the total number of labeled neurons differed between the groups was not determined. Like those in the PG, DRG satellite cells adjacent to neurons (Fig. 4A, B), Schwann cells among nerve trunks, and axon-rich nerve trunks in the ganglia (Fig. 4D, F), or connective tissue cells of the DRG and NG capsule did not show silver grains above background level.

ER-β mRNA-expressing neurons in ganglia

PG neurons expressing ER-β mRNA were evident in autoradiograms as lightly to moderately labeled neurons (Fig. 5A). The ER-β mRNA-expressing neurons were similar in number (per ganglion) to those showing ER-β immunoreactivity by immunohistochemistry. Sensory neurons of DRG and NG also expressed ER-β mRNA. For the most part, neurons with the most dense labeling were medium in size (Fig. 5B), though some small-size neurons were moderately labeled (Fig. 5C), and occasionally large neurons were lightly positive. In DRG, there were approximately six to ten ER-β mRNA-expressing neurons per ganglion section that were densely

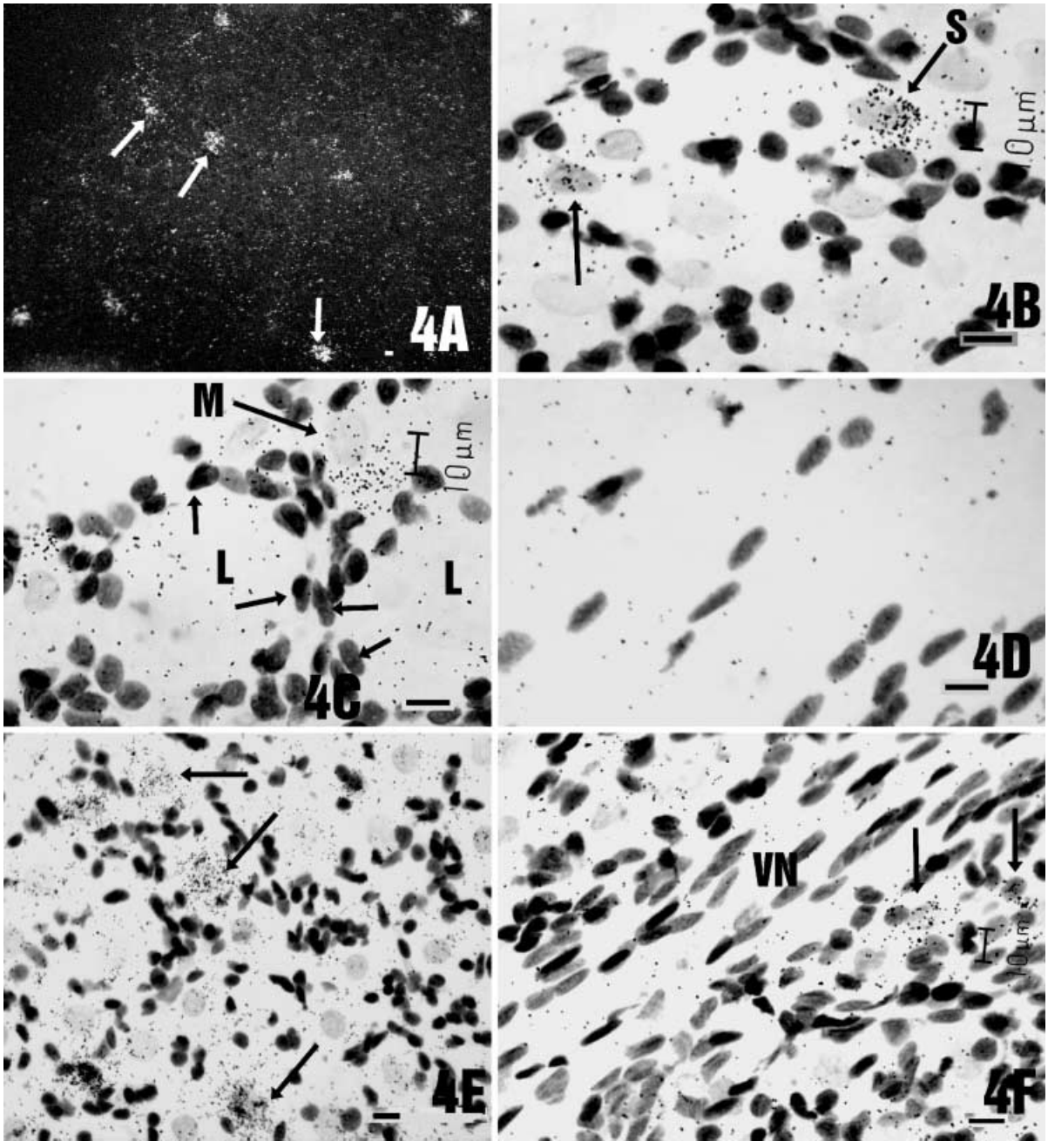

Fig. 4A–F Sections from the DRG (**A–D**) and NG (**E, F**) of an ovariectomized rat (**A–E**) and an intact rat (**F**) processed for in situ hybridization autoradiography for ER-α mRNA. **A** was photographed at low magnification with darkfield optics and shows several ER-α mRNA-positive neurons (*arrows*), but details and characteristics of the neurons are not discernible. **B** Shows, at higher magnification with brightfield optics, a moderately labeled, small sensory neuron (*S*, adjacent to the 10-µm marker) and a lightly labeled, small neuron (*arrow*). Note that the Schwann and satellite cells are not labeled. **C** A medium-sized neuron (*M*) is moderately labeled, but large neurons (*L*) and surrounding satellite cells (*arrows*) are not labeled. **D** A bundle of axons coursing through the DRG, showing the average level of control background silver grains overlying nonperikaryal cytoplasm for comparison with positive labeling of neurons. **E** NG section showing several moderately labeled perikarya (*arrows*) from an ovariectomized rat. **F** Small neurons (*arrows*) lightly labeled for ER-α mRNA in the NG from an intact rat. Note the low level of background silver grains overlying vagal nerve fibers (*VN*) coursing through the ganglion. *Bar* 10 µm

labeled (Fig. 5C), whereas many more were lightly labeled, medium- and large-sized neurons (Fig. 5B). Furthermore, fewer neurons (four to six neurons per section) expressed ER-β mRNA in the NG (Fig. 5D, E) than in the DRG.

Satellite cells adjacent to neurons, Schwann cells among nerve trunks in the ganglia (Fig. 5E), or connective tissue cells of the ganglion capsule did not contain silver grains in numbers above background level.

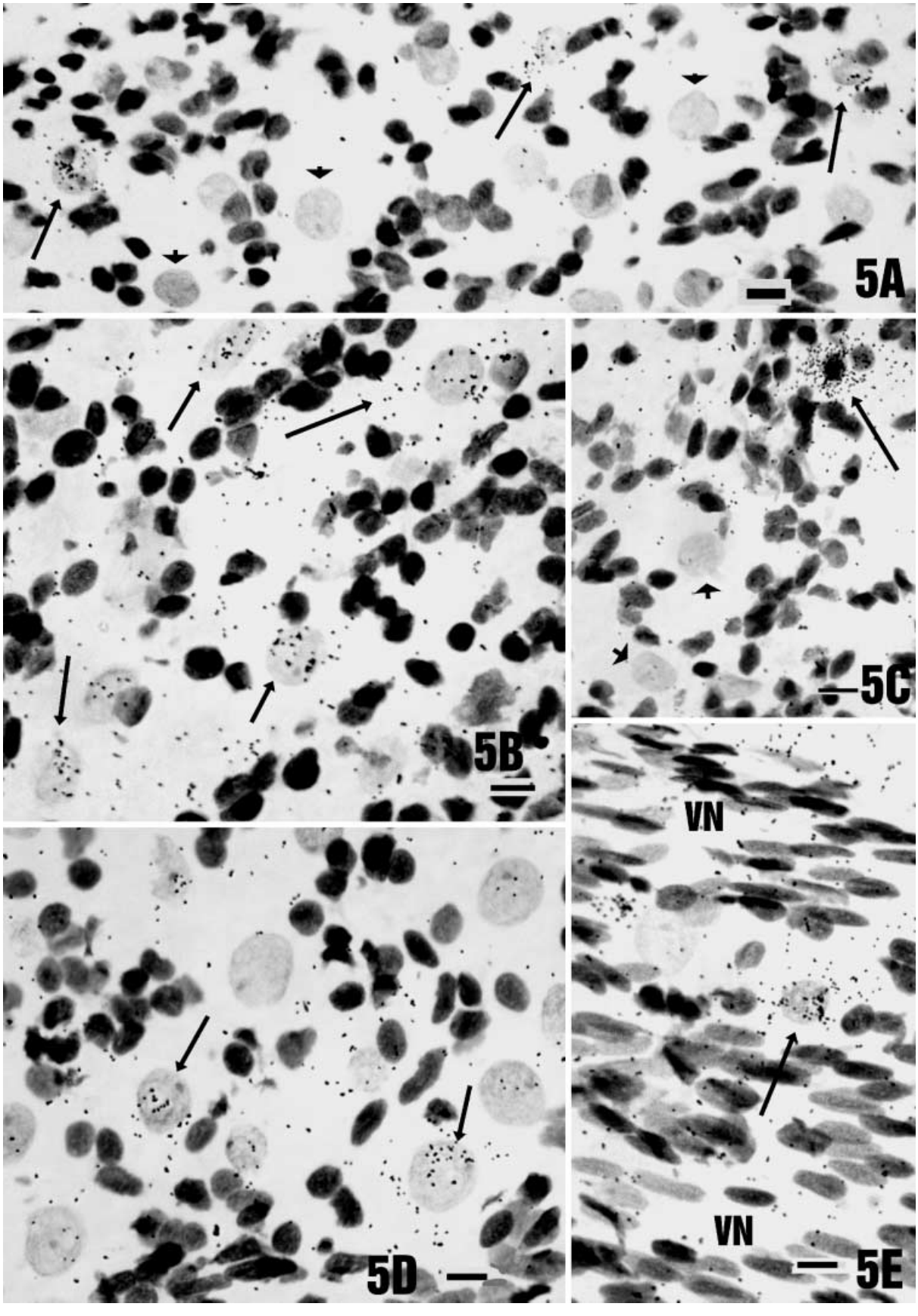
5A
5B
5C
VN
5D
VN
5E

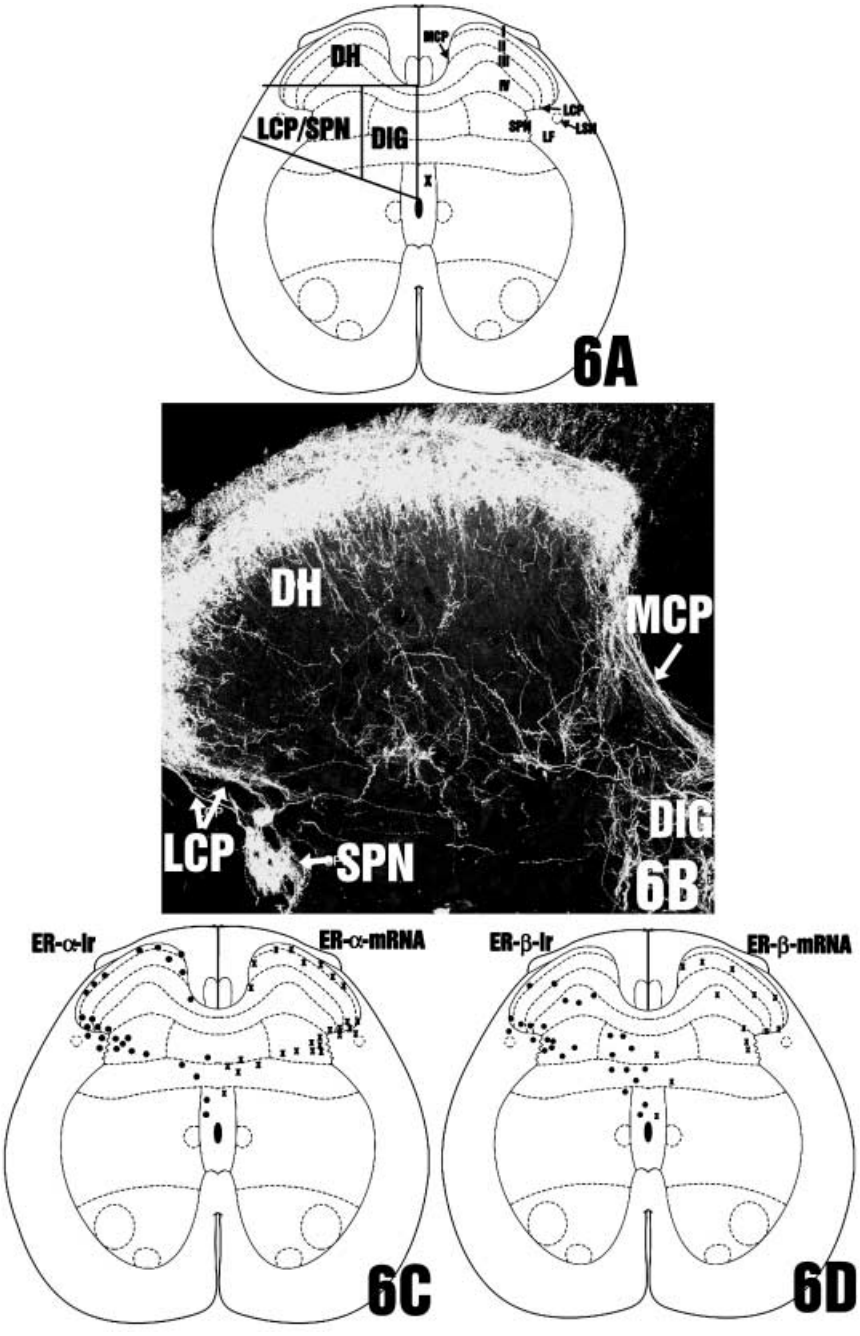

Fig. 6A–D Orientation diagrams of the L6-S1 spinal cord for counting of neurons (**A**), distribution of primary sensory nerves terminals (**B**), distribution of ER-α neurons (**C**), and ER-β (**D**) neurons. **A** S1 of the spinal cord (modified from Paxinos and Watson 1997). The areas in which the ER-positive cells were counted are shown on the *left* and labeled *DH* (dorsal horn), *LCP/SPN* (lateral collateral pathway/sacral parasympathetic nucleus), and *DIG* (dorsal intermediate gray). In addition, for orientation, the numbered dorsal horn laminae according to Rexed are labeled on the *right*, as well as the location of the medial collateral pathway (*MCP*), lateral collateral pathway (*LCP*), sacral parasympathetic nucleus (*SPN*), lateral funiculus (*LF*), and lateral spinal nucleus (*LSN*). **B** Orientation photograph of the left, upper quadrant of the lumbosacral spinal cord similar to an area in **A**, showing the dorsal horn (*DH*), medial collateral pathway (*MCP*), lateral collateral pathway (*LCP*), sacral parasympathetic nucleus (*SPN*), and dorsal intermediate gray (*DIG*) dorsal to the central canal. The section was immunostained for calcitonin gene-related peptide (CGRP) to show areas of termination of primary afferent nerve fibers that are immunoreactive for CGRP in the *DH*, fibers coursing to the *SPN* in the *LCP*, and fibers coursing to the *DIG* in the *MCP*. **C, D** Schematics (modified from Paxinos and Watson 1997) of the distribution of ER-α-immunoreactive neurons (*Ir*; *filled circles*) on the *left* (**C**), ER-α-mRNA (*X*) on the *right* of **C**; ER-β-immunoreactive neurons (*filled circles*) on the *left* (**D**), and ER-β-mRNA (*X*) on the *right* of **D**. These diagrams reflect the number of labeled neurons in two representative spinal cord sections and each symbol represents one neuron

◀ **Fig. 5A–E** Sections from the PG (**A**), DRG (**B, C**), and NG (**D, E**) processed for in situ hybridization autoradiography for ER-β mRNA. **A** Section of the PG showing a few lightly labeled, ER-β mRNA-positive neurons (*arrows*) among many unlabeled neurons (*arrowheads*). **B** Several lightly labeled DRG neurons (*arrows*). **C** shows a small, intensely labeled DRG neuron (*arrow*) near several unlabeled medium-to-large neurons (*arrowheads*). **D** Lightly labeled ER-β mRNA-positive sensory neurons (*arrows*) in the NG. **E** An ER-β mRNA-positive neuron (*arrow*) among many unlabeled vagal nerve fibers (*VN*). The VN reflects the background level of silver grains overlying nonperikaryal tissue in the NG as an illustration of the control level of label. *Bar* 10 μm

Spinal cord orientation and CGRP

For orientation purposes, a section of the L6-S1 spinal cord is shown in Fig. 6A, with the areas outlined for counting of cells and to show terminology used. A similar section was immunostained with an antiserum against CGRP (Fig. 6B). Since CGRP is present almost exclusively in terminals of primary afferent axons from DRG neurons (Traub et al. 1989; Villar et al. 1991), this proved useful to highlight specific areas of the spinal cord where peripheral sensory nerve fibers course and terminate. In this way, ER-containing neurons could be

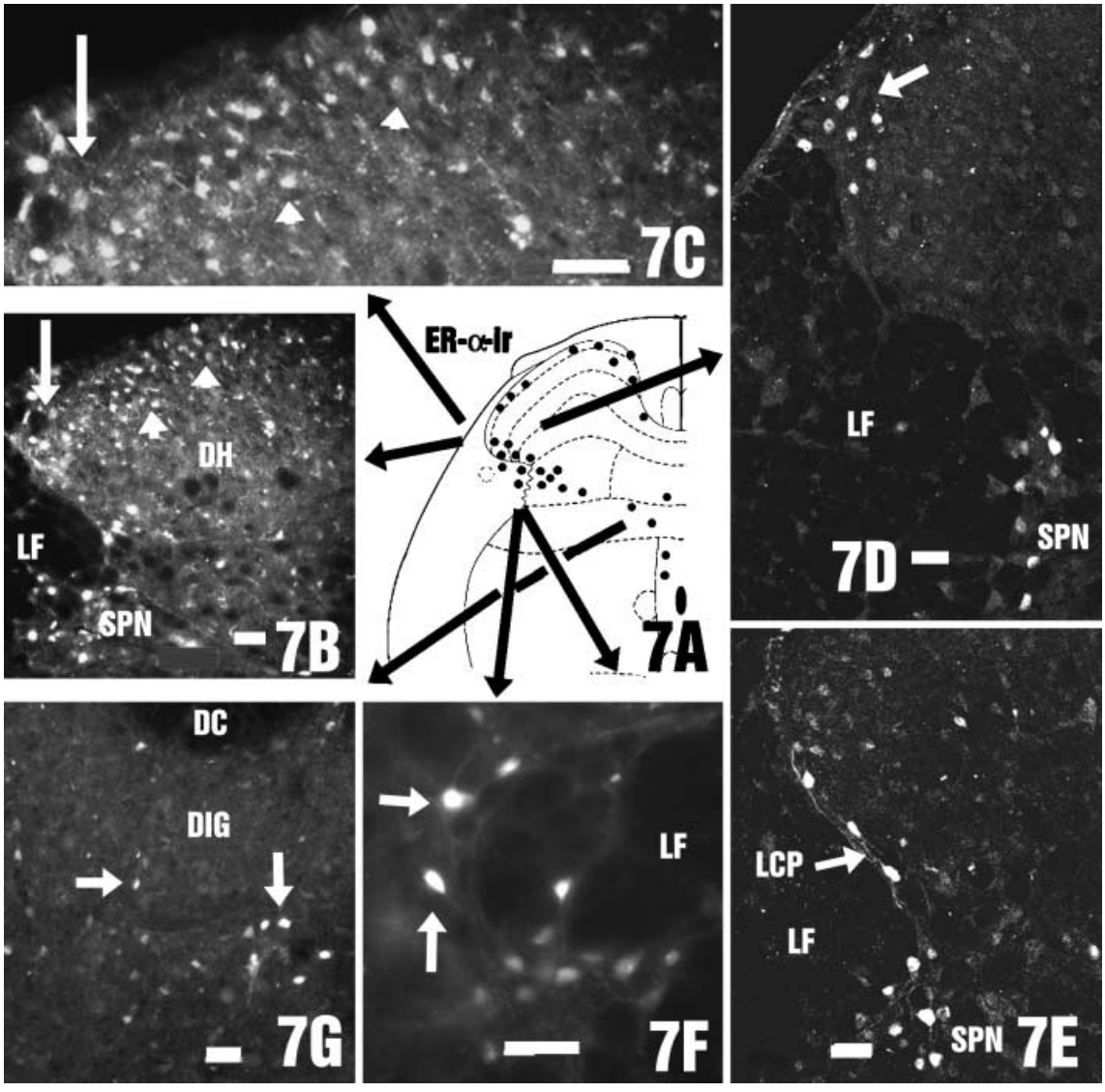

Fig. 7A–G Sections of the lumbosacral spinal cord of an ovariectomized rat immunostained for ER-α. **A** Summary of the distribution of ER-α-immunoreactive neuronal nuclei, where *arrows* link areas to representative micrographs. **B** Low-magnification view of ER-α-immunoreactive neurons (*arrowheads*) scattered in the outer laminae of the dorsal horn (*DH*), clustered in the lateral DH (*arrow*) and in the sacral parasympathetic nucleus (*SPN*) near the lateral funiculus (*LF*). **C** Higher-magnification view of ER-α-immunoreactive neurons of Fig. 7**B** in the outer laminae of the DH. **D** A cluster (*arrow*) of ER-α-immunoreactive neurons in the lateral DH. In addition, immunoreactive cells are also seen in the *SPN* (*LF* lateral funiculus). **E** Examination of adjacent sections allows one to determine that there is a continuum of ER-α-immunoreactive neurons from the lateral DH (see *arrow* in Fig. 7**D**), along the lateral collateral pathway (*LCP*) to the *SPN*. **F** Higher-magnification view of presumed preganglionic parasympathetic neurons in the SPN (*arrows*). **G** Labeled neurons (*arrows*) in the dorsal intermediate gray (*DIG*) between the dorsal columns (*DC*) and the central canal (not seen). *Bar* 50 μm

Table 3 Mean numbers of ER-immunoreactive neurons and ER mRNA-expressing neurons in the dorsal half of the L6-S1 spinal cord segments of ovariectomized rats (*DH* dorsal horn, *SPN/LCP* lateral collateral pathway and leading down to sacral parasympathetic nucleus, *DIG* dorsal intermediate gray and area dorsal to the central canal)

Area	Mean number of ER-immunoreactive cells per section[a]		Mean number of ERmRNA-expressing cells per section[a]	
	ER-α	ER-β	ER-α	ER-β
DH	4.7	2.6	4.2	3.0
SPN/LCP	7.0	6.2	7.1	2.6
DIG	2.3	5.4	2.7	1.3
Mean total cells/section	14.0	14.2	14.0	6.9

[a] Representative sections were 40 μm thick

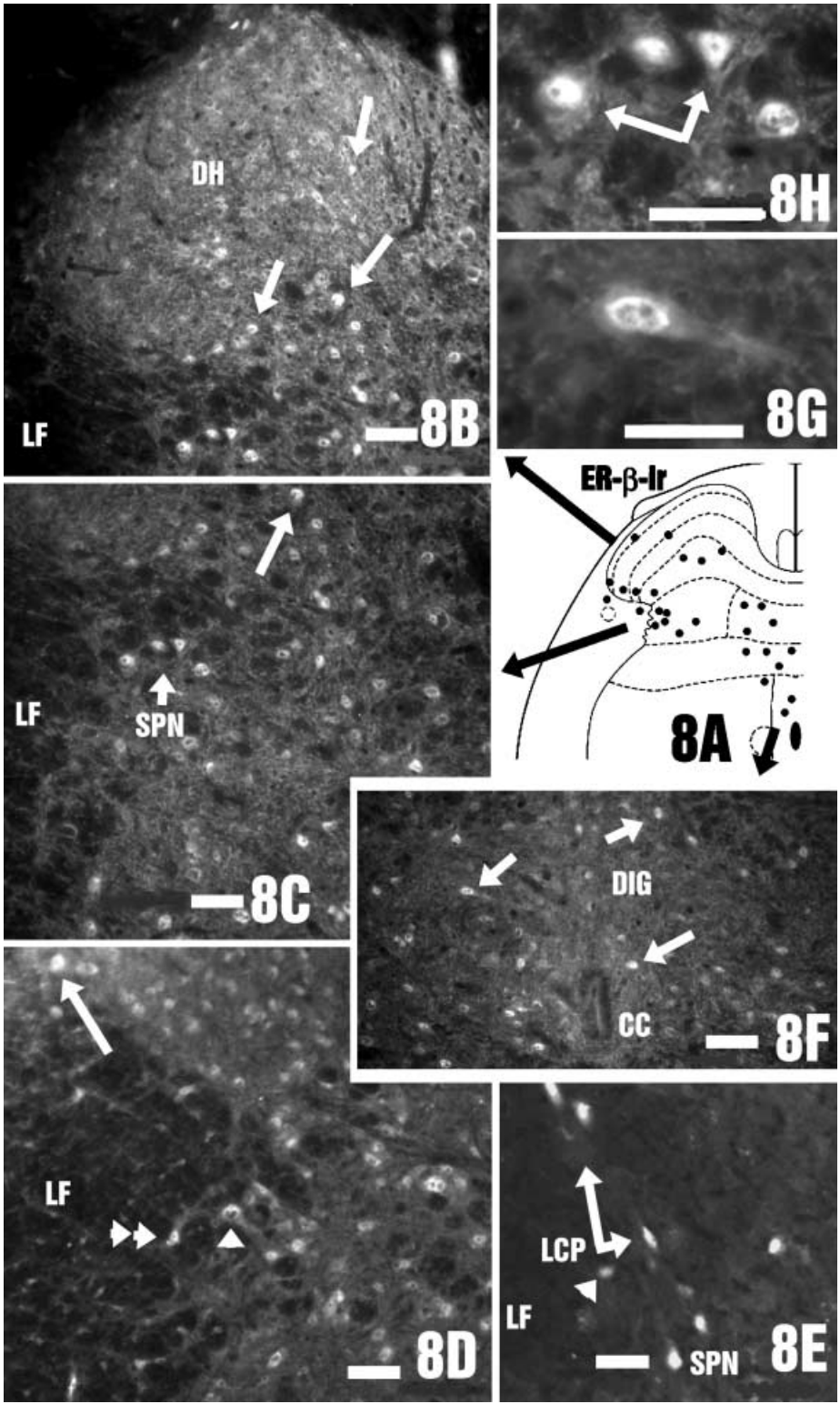

Fig. 8A–H Cryostat sections of the lumbosacral spinal cord of an ovariectomized rat immunostained for ER-β. **A** summarizes the distribution of ER-β-immunoreactive neuronal nuclei and the *arrows* link areas to representative micrographs. **B** Low-magnification view of ER-β-immunoreactive neurons (*arrows*) scattered in the deeper laminae of the dorsal horn (*DH*), with few in the outer laminae (*LF* lateral funiculus). **C** Higher-magnification view of **B**, showing ER-β-immunoreactive neurons in the deep DH (*arrow*) and sacral parasympathetic nucleus (*SPN*; *arrowhead*). **D** ER-β-immunoreactive neurons in the lateral DH (*arrow*), SPN (*arrowhead*), and lateral funiculus (*LF*, double *arrowhead*). **E** A continuum of ER-β-immunoreactive neurons from the lateral DH (see *arrow* in **D**), along the lateral collateral pathway (*LCP*; *arrow*) to the SPN. Occasional neurons were evident in the lateral funiculus (*LF*; *arrowhead*). **F** Labeled neurons (*arrows*) in the dorsal intermediate gray (*DIG*) between the dorsal columns (not seen) and the central canal (*CC*). **G, H** Higher-magnification view of fusiform neurons in the area between the SPN and DIG (**G**) and stellate-shaped, presumed preganglionic parasympathetic, neurons in the SPN (*arrows* in **H**). *Bar* 50 μm

related to the locations of sensory and autonomic areas of the spinal cord. CGRP immunoreactivity is heavily concentrated in the outer laminae I and II of the dorsal horn, along the medial collateral pathways (MCP) and LCP, in the SPN, DIG above the central canal, and in lamina X around the central canal (Fig. 6B). Thus, these fibers paralleled the distribution of sensory fibers from the reproductive organs (Kawatani et al. 1990), and those in the LCP are directed to the autonomic areas such as the SPN (Morgan et al. 1981). Summary diagrams outlining the distribution of ER-α- and β-immunoreactive neurons and ER-α mRNA-expressing and ER-β mRNA-

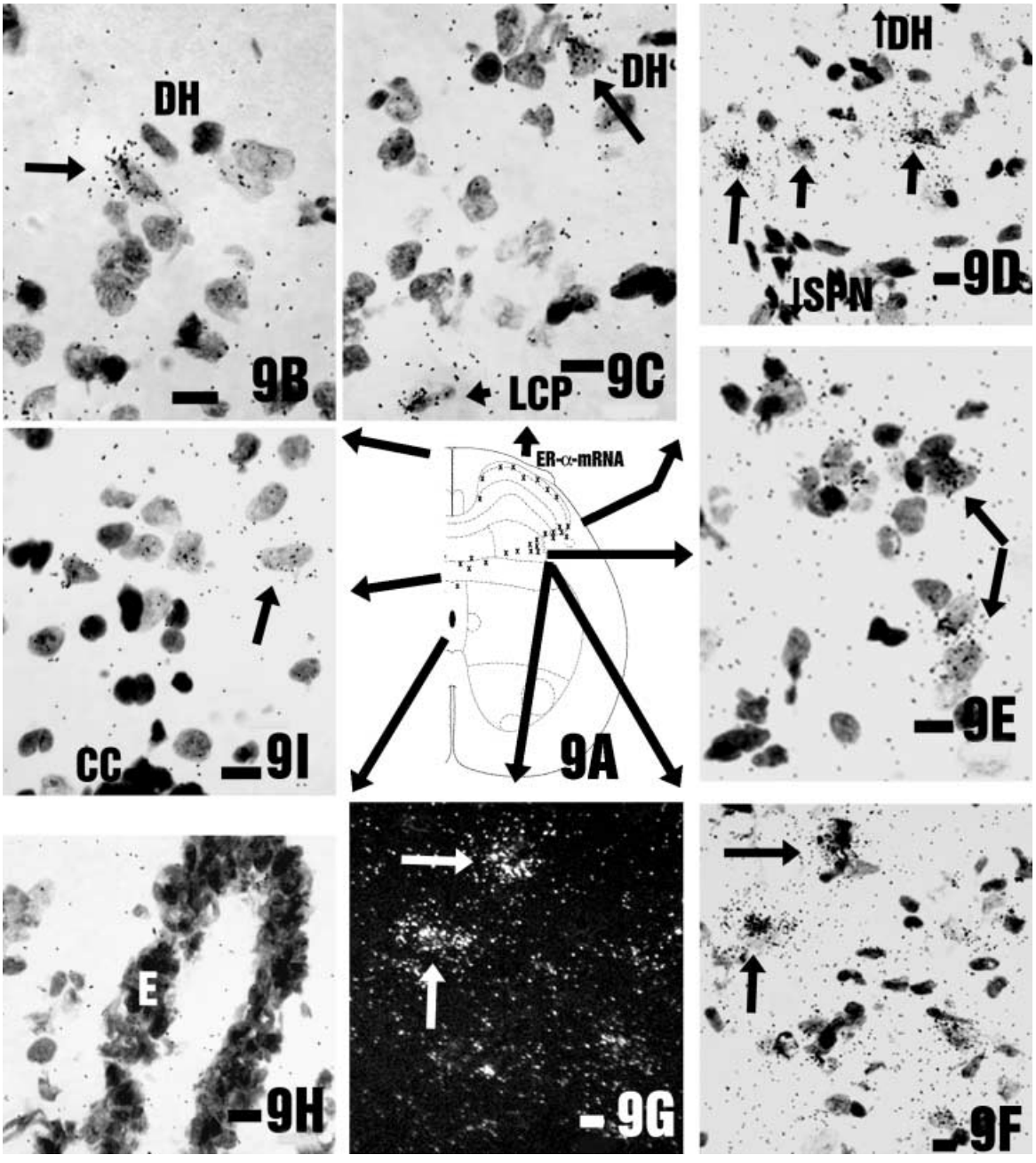

Fig. 9A–I Autoradiograms of the lumbosacral spinal cord of an ovariectomized (**B–D, F, H**) and intact (**E**, **I**) rats processed for ER-α mRNA by in situ hybridization. **A** summarizes the distribution of ER-α-mRNA-positive neurons and the *arrows* link areas to representative micrographs. **B** Low-magnification view of ER-α-mRNA-containing neurons (*arrow*) scattered in the outer laminae of the dorsal horn (*DH*). **C** Labeled neurons in the lateral DH (*arrow*) and in the lateral collateral pathway (*LCP*; *arrowhead*). **D** Several labeled neurons (*arrow*) in the LCP. (*↓SPN* Direction of the sacral parasympathetic nucleus, *↑DH* direction of the outer laminae of the DH.) **E** Moderately labeled neurons (*arrows*) in the SPN of an intact rat. **F** Brightfield micrograph showing intensely labeled neurons (*arrows*) in the SPN of an ovariectomized rat. **G** As **F**, but photographed with darkfield optics, which enhance the visibility of labeled neurons in the SPN. **H** The absence of ER-α mRNA-specific labeling in the ependyma (*E*) of the central canal. **I** Lightly labeled neurons (*arrows*) are in lamina X dorsal to the central canal (*CC*) from an intact rat. *Bar* 10 µm

expressing neurons in the spinal cord are presented in Fig. 6C, D.

ER-α immunoreactivity in spinal cord

A summary of the distribution of ER-α-containing neurons is shown in Fig. 7A. These neurons in the spinal cord were distributed largely in outer laminae (I and II) of the dorsal horn (Fig. 7A–C) and in the SPN (Fig. 7D–F). Concentrations of ER-α-positive neurons were regularly evident at the lateral margin of the dorsal horn (Fig. 7B–D). Immunoreactive neurons were common along the lateral and medial margins of the dorsal horn in the area of the MCP and LCP (Fig. 7E). From the

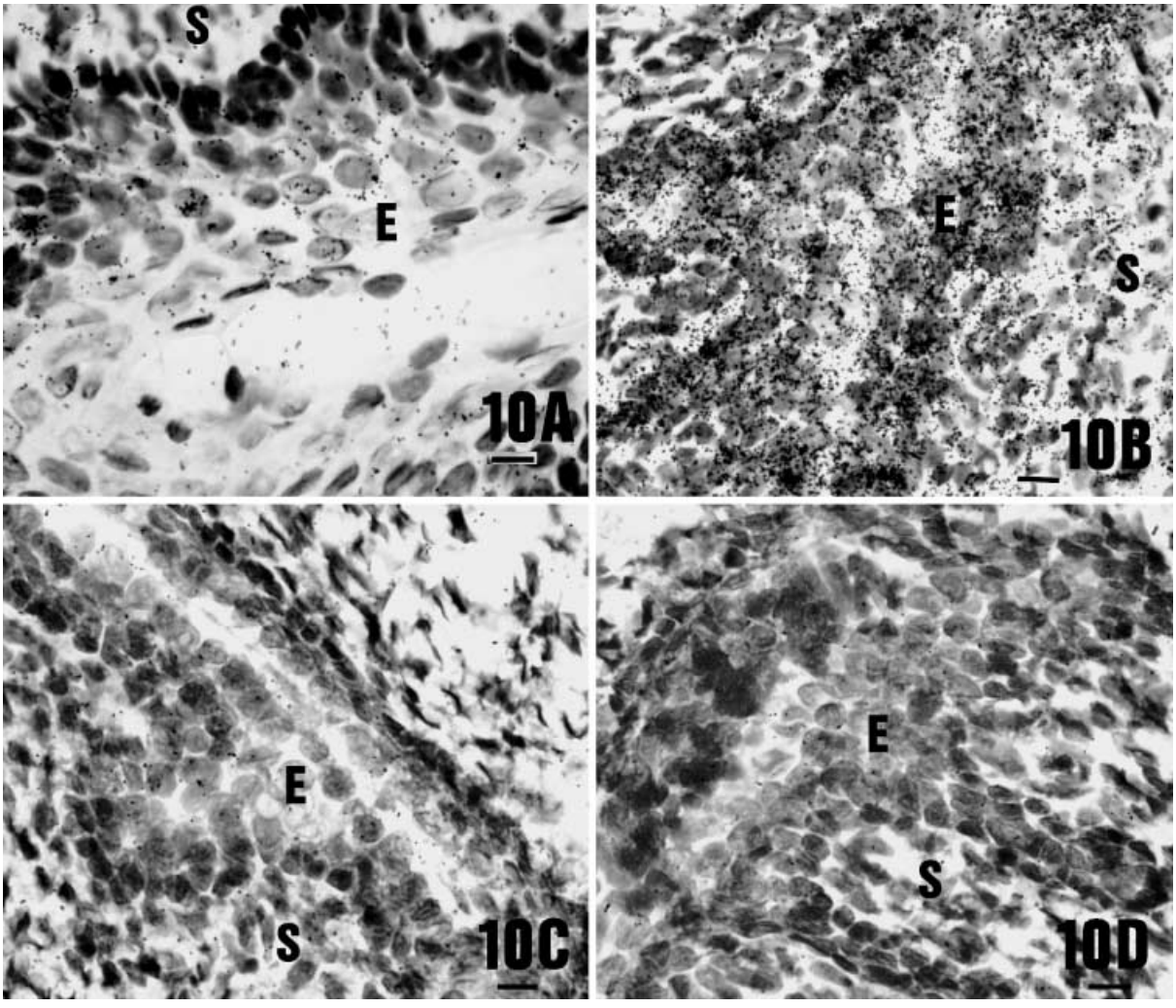

Fig. 10A–D Autoradiograms of the uterine cervix from intact (**A, C**) and ovariectomized (**B, D**) rats processed for demonstration of ER-α mRNA (**A, B**) and ER-β mRNA (**C, D**). **A** Light labeling of ER-α-mRNA over the epithelial cells (*E*) and stroma (*S*) of the uterine cervix of an intact rat. **B** Relatively dense labeling for ER-α mRNA over the epithelium (*E*) and stroma (*S*) in an ovariectomized rat compared with the intact rat (**A**). **C, D** Almost no labeling for ER-β-mRNA in the uterine cervix and no apparent differences between an intact rat (**C**) and an ovariectomized rat (**D**). (*E* Epithelium, *S* stroma.) *Bar* 10 µm

LCP, labeled neurons could be traced ventrally to the SPN (Fig. 7D,E). Abundant ER-α-immunoreactive neurons were distributed across the DIG of the spinal cord largely in and around lamina X near the central canal (Fig. 7G). A few ER-α-immunoreactive neurons were regularly evident in the lateral funiculus (LF) near the lateral spinal nucleus. Counts of ER-α-immunoreactive neurons in L6-S1 spinal cord sections of ovariectomized animals revealed an average of 14.0 neurons per 40-µm-thick section (Table 3).

The distribution of ER-α-immunoreactive neurons closely paralleled the distribution of CGRP-immunoreactive primary afferent nerve fibers and terminals – most notably laminae I–II of the dorsal horn, along the LCP and MCP, in the DIG, SPN, and lamina X (Figs. 6B, 7).

ER-β immunoreactivity in spinal cord

A summary of the distribution of ER-β-containing neurons is shown in Fig. 8A, and these neurons had a similar distribution pattern and number in the spinal cord to the ER-α-immunoreactive neurons (Figs. 6C, D, Table 3). ER-β-immunoreactive neurons were present in the dorsal horn (but mainly deeper layers II–V; Fig. 8A, B), LCP (Fig. 8E), MCP, SPN (Fig. 8C), lateral funiculus (Fig. 8D, E), and DIG (Fig. 8F). In general, it appeared that ER-β-immunoreactive neurons were more deeply placed in the dorsal half of the spinal cord than were ER-α-immunoreactive neurons. Within the SPN of the L6-S1 cord, the ER-β-positive neurons were stellate in shape (Fig. 8H) and fusiform ER-β-positive neurons were evident in the intermediate gray between the SPN and central canal (Fig. 8G). Furthermore, occasional ER-β-immunoreactive neurons, unlike ER-α neurons, were present in the ventral horn, mainly in the dorsomedial aspect of the ventral horn (not shown).

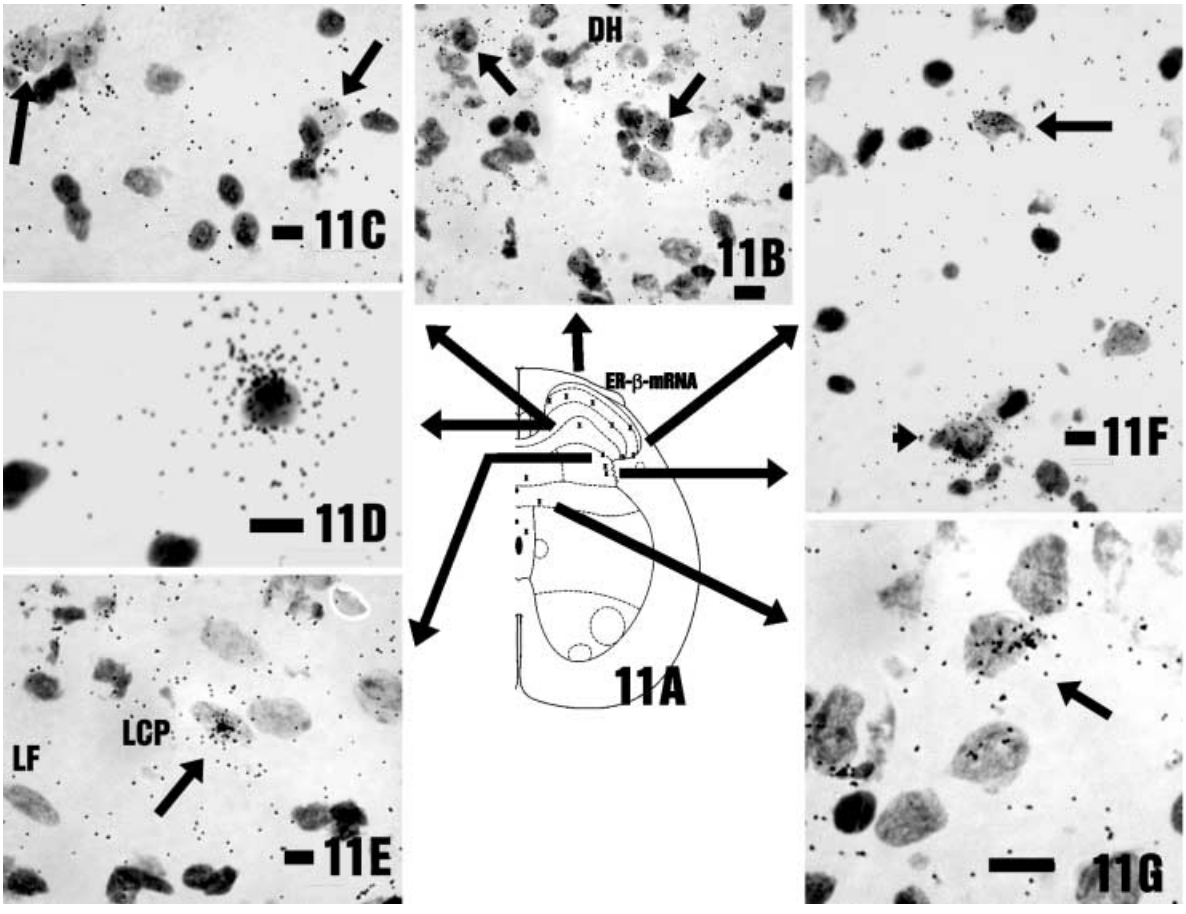

Fig. 11A–G Autoradiograms of the lumbosacral spinal cord processed for ER-β mRNA by in situ hybridization. **A** summarizes the distribution of ER-β-mRNA-positive neurons and the *arrows* link areas to representative micrographs. **B** A few lightly labeled ER-β-mRNA-containing neurons (*arrow*) scattered in the outer laminae of the dorsal horn (*DH*). **C** ER-β mRNA-positive neurons (*arrows*) in the deep dorsal horn. **D** A high-magnification view of an intensely labeled neuron in the deep DH. **E** An ER-β mRNA-positive neuron (*arrow*) in the lateral collateral pathway (*LCP*) (*LF,* lateral funiculus). **F** Labeled neurons in the deep dorsal horn (*arrow*) and the sacral parasympathetic nucleus (SPN; *arrowhead*). **G** ER-β mRNA-containing neurons (*arrow*) were frequent in the dorsal intermediate gray (DIG) between the dorsal columns (not seen) and the central canal. *Bar* 10 μm

ER-α mRNA-expressing neurons in spinal cord

Most perikarya that expressed ER-α mRNA were evident in autoradiograms as lightly to moderately, and occasionally densely, labeled neurons in specific areas of the spinal cord. Their distribution pattern is summarized in Fig. 9A and was similar to that of neurons showing ER-α immunoreactivity (Fig. 6C). For example, ER-α mRNA-expressing neurons occupied the outer dorsal horn (lamina I–II; Fig. 9B, C), the dorsolateral part of the dorsal horn (Fig. 9C), the LCP (Fig. 9C, D), MCP, SPN (Fig. 9E, F, G), DIG, and lamina X (Fig. 9I). The number (per section) of ER-α mRNA-expressing neurons from ovariectomized rats was similar to that for ER-α-immunoreactive neurons as evident from immunohistochemistry, 13.95 compared with 14.0, respectively (see Table 3). Though, we have not yet quantitated any differences, our impression was that spinal cord neurons from ovariectomized rats were more heavily labeled by silver grains for ER-α mRNA expression than those from intact rat.

When areas that lacked neuronal perikarya such as the ependymal lining of the central canal, dorsal root entry zone, dorsal columns, and lateral funiculus were examined, the number of silver grains (i.e., labeling) did not appear greater than background numbers (Fig. 9H). In addition, autoradiograms from hybridized sections of the uterine cervix showed intense labeling of the endocervix for ER-α mRNA-expressing neurons in the ovariectomized rat (Fig. 10B), but much less intense signal from endocervix of the intact rat (Fig. 10A).

ER-β mRNA-expressing neurons in spinal cord

The overall distribution of ER-β mRNA-expressing neurons in the L6-S1 segments of the spinal cord was similar to that for ER-β-immunoreactive neurons and is summarized in Figure 6D. For example, these ER-β mRNA-expressing neurons were present in the dorsal horn (Fig. 11A–D, F), LCP (Fig. 11E), MCP, SPN (Fig. 11F), lamina X, and DIG (Figs. 6D, 11G; see Table 3). In gen-

eral, ER-β mRNA-expressing neurons were in deeper dorsal horn laminae more so than in outer laminae. The number (per section) of ER-β mRNA-expressing neurons from ovariectomized rats was smaller than that for ER-β-immunoreactive neurons as evident from immunohistochemistry, 6.83 compared with 14.20, respectively (see Table 3). We did not discern any differences in labeling by silver grains for ER-β mRNA expression in spinal cord neurons from ovariectomized compared with intact rats; however, we have not yet quantitated any differences.

On examination of areas that lacked neuron somata such as the ependymal lining of the central canal, dorsal root entry zone, dorsal columns, and lateral funiculus, the numbers of silver grains did not appear higher than background level. In addition, autoradiograms from hybridized sections of the uterine cervix showed only very light signal in the endocervix for ER-β mRNA (relative to ER-α mRNA), whether sections were obtained from intact or ovariectomized rats (Fig. 11C, D). This coincides with the report of very low ER-β transcript in the (mouse) uterine cervix (Couse and Korach 1998).

Discussion

The classic form of ER is the α-isoform, and its distribution and functional attributes in the CNS have received considerable attention (Matsumoto et al. 1988; Simerly et al. 1990; Li et al. 1993; Rissman et al. 1997; Mufson et al. 1999). Fewer studies have focused on ER-α in peripheral neurons (Papka et al. 1997; Yang et al. 1998; Liuzzi et al. 1999a, 1999b; Patrone et al. 1999; Taleghany et al. 1999). Furthermore, since revelation of a second isoform of ER, ER-β (Kuiper et al. 1996, 1998; Mosselman et al. 1996; Tremblay et al. 1997), several studies have detailed the distribution of ER-β in the CNS (Shughrue et al. 1996a, 1997, 1998b, 1999, 2000; Li et al. 1997), but only one has examined ER-β (mRNA) in the spinal cord (Shughrue et al. 1997) and ER-β (mRNA) in peripheral sensory ganglia (Taleghany et al. 1999). Thus, the importance of this study is that it is the first to identify both ER-β protein and mRNA transcripts in the neurons of the lumbosacral spinal cord and in peripheral autonomic and sensory ganglionic neurons related to female reproductive organs. Additional important aspects of this study were the comparison of ER-α-immunoreactive and ER-β-immunoreactive neurons in these ganglia and in the spinal cord and that ganglionic neurons expressing ER-α and -β project axons to the uterus and cervix. Consequently, estrogens could have a complex influence on structural and/or functional aspects of neural circuits involving these neurons and thus their target structures, e.g., reproductive organs.

The autonomic and sensory nerve supply to the uterus and uterine cervix, indicating the sources of, functions of, and neurotransmitter used by these fibers, has been detailed (Berkley et al. 1988, 1993a, 1993b; Papka and Traurig 1993; Traurig and Papka 1993; Papka and Shew 1994; Houdeau et al. 1998). Furthermore, some uterine-related neurons are responsive to estrogens through ER-α (Papka et al. 1997). Our current results extend these findings by showing that uterine-related PG and DRG neurons also can be influenced through ER-β; preliminary data from our laboratory indicates that ER-α and ER-β may coexist in the some sensory neurons.

Neurons of the female PG appear to respond to gonadal steroid hormones. For example, Coujard (1951) has shown that ovariectomy decreases the volume of PG neurons and that subsequent estrogen treatment is restorative. According to Schleicher et al. (1985), about 25% of mouse PG neurons bind estradiol. Since ER-α/-β localization is clearly nuclear, this suggests that estrogens have genomic effects in these neurons by hormone ligand-receptor complex binding to an estrogen response element of the DNA and modulate transcription of target genes (Murdoch and Gorski 1991). Such effects could involve protein synthetic activity and help explain the volume changes reported by Coujard (1951). In addition, Gollapudi and Oblinger (1999a) have shown that ER-α is present in PC12 cells [neural crest derivatives that are nerve growth factor (NGF)-dependent] and that estrogens have cytoprotective (cell survival) effects that involves NGF and the antiapoptotic molecule Bcl-X_L (Gollipudi and Oblinger 1999b). Furthermore, estrogens stimulate neurotransmitter levels (in CNS neurons; Gibbs et al. 1994; Okamura et al. 1994a, 1994b; Yuri and Kawata 1994; Dufourny and Warembourg 1999; Miller et al. 1999), upregulate neuronal-nitric oxide synthase in autonomic and/or sensory nerves in the vagina (Berman et al. 1998), or downregulate CGRP in sensory neurons (Moussaoui et al. 1996; Duval et al. 1998; Yang et al. 1998). These types of regulation could occur in peripheral autonomic and sensory neurons that innervate the uterus. ER-α and ER-β may be differentially regulated in different tissues including the CNS (Osterlund et al. 1998; Belcher 1999) and DRG (Taleghany et al. 1999). Whether or not the ERs are differentially regulated in the autonomic neurons of the PG is currently not known. It is noteworthy that other studies have indicated different preferences in binding of estrogenic substances to ER-α compared with ER-β (Kuiper et al. 1997, 1998), different roles of ER-α and -β in regulating viscera (Campbell-Thompson 1997), and neuronal characteristics with regard to neurite sprouting (Patrone et al. 2000). For example, 17-β-estradiol acting through ER-α induces increased length and number of neurites, whereas ER-β activation modulates only neurite length.

The presence of ER-α immunoreactivity and ER-α mRNA in sensory neurons of DRG was first reported by Sohrabji et al. (1994). That study implicates estrogens, working through ER-α, as modulators of NGF receptor expression and suggests that estrogen mediates NGF-dependent neuronal plasticity and repair. This is interesting in view of the fact that both peripheral autonomic and sensory neurons are NGF-dependent (Barde 1989; Mendell 1994). Furthermore, estrogen regulates neurofilament gene expression in DRG neurons and influences

the maintenance and function of primary sensory neurons (Scoville et al. 1997). In fact, long-term estrogen treatment of ovariectomized rats reduces levels of trkA NGF receptor mRNA and β-preprotachykinin mRNA (Liuzzi et al. 1999a), whereas short-term treatment has the opposite effect. Furthermore, Patrone et al. (1999) have shown that 17-β-estradiol, working through ER-α and ER-β in developing DRG neurons, increases the survival of neurons deprived of NGF and promotes the expression of the antiapoptotic molecule Bcl-x. Taken together, these studies suggest that both ERs are important in the survival and maintenance of DRG neurons as well as expression of peptide transmitters. Indeed, Yang et al. (1998) have shown that the number of CGRP-immunoreactive DRG neurons increases after ovariectomy and decreases with subsequent estradiol treatment, leading to the conclusion that CGRP expression is downregulated by estrogens through the ER. CGRP is expressed by many small- and intermediate-sized nociceptive neurons (Lee et al. 1985; Papka and McNeill 1992b; Yang et al. 1998), which are sensitive to the sensory neurotoxin capsaicin (Holzer 1988; Papka and Traurig 1989). Such capsaicin-sensitive neurons must possess the capsaicin receptor VR1(Caterina et al. 1997; Guo et al. 1999); indeed some ER-α-immunoreactive and ER-β-immunoreactive DRG neurons are VR1-positive. Consequently, some VR1-immunoreactive/ER-containing neurons could be classified as nociceptive neurons that convey information from the reproductive organs to the spinal cord or have "efferent" functions in end-organ tissues, e.g., neurogenic inflammation (Holzer 1988).

Several studies indicate that sensitivity of peripheral nerves varies with the estrous cycle (changing estrogen levels; Berkley et al. 1988; Robbins et al. 1992), including receptive fields (Komisaruk et al. 1972; Kow and Pfaff 1973; Adler et al. 1977). In this regard, Taleghany et al. (1999) have revealed that expression of both ER-α and ER-β mRNAs in L6-S1 DRG neurons fluctuates with estrogen levels in the estrous cycle. Whether ER-α or ER-β influences the transmitter content of DRG neurons and their excitability is of considerable interest to our laboratory with regard to uterine innervation, as this innervation expresses plasticity during the estrous cycle and pregnancy (Sporrong et al. 1981; Alm et al. 1988; Lundberg et al. 1988; Zoubina and Smith 2000; Brauer et al. 2000). The presence of ER-α and ER-β isoforms in PG and DRG neurons suggests that both receptors play roles in mediating the action of estrogens in these neurons. Two isoforms of the receptor in ganglionic neurons, whether in the same or different cells, suggests complex control mechanisms for estrogens in the ganglia.

Visceral afferent neurons of the vagus nerve, located in the NG, also contained ER-α and ER-β mRNAs and protein. Their central processes largely project into the nucleus of the tractus solitarius. Of all areas of the caudal brainstem, the visceral nucleus of the tractus solitarius has the greatest number of ER-α mRNA (Simerly et al. 1990; Shughrue et al. 1997), ER-β mRNA (Shughrue et al. 1997), and ER-α-immunoreactive (Papka et al. 1998) neuronal somata. Accumulating neuroanatomical, physiological, and behavioral data suggest the uterus receives a vagal input (Collins et al. 1999). Thus, estrogen-responsive neural circuits may exist between the uterus and brainstem.

ER-α-immunoreactive and ER-β-immunoreactive neurons have similar numbers and distributions in the lumbosacral spinal cord, except in the dorsal horn, where ER-α-immunoreactive neurons tended to be more numerous in the outer laminae (I and II); whereas ER-β-immunoreactive neurons tended to be more numerous in deeper laminae. This agrees with previous studies which reported the distribution of ER-α (Simerly et al. 1990; Amandusson et al. 1995, 1996; Williams and Papka 1996; Shughrue et al. 1997) and ER-β mRNA-containing neurons (Shughrue et al. 1997) in the spinal cord dorsal horn. Our results showed a concentration of ER-containing neurons, particularly ER-α-immunoreactive neurons, not only in the outer laminae but also in the dorsolateral part of the dorsal horn. Neurons in this location could be spinothalamic (Willis et al. 1978). Furthermore, ER-positive neurons extended from this location along the LCP, where they seemingly continued to the SPN. Many SPN neurons are preganglionic to the PG; thus autonomic pathways to the pelvic organs contain ER and could be influenced by estrogens. ER neurons were conspicuous in the DIG area between the central canal and the dorsal columns; such areas are rich in neurons with ascending projections that respond to cutaneous and visceral afferent inputs (Nahin et al. 1983; Honda 1985). Thus, estrogens could influence ascending circuits. Neurons expressing ER-α-mRNA and ER-α immunoreactivity and ER-β mRNA and ER-β immunoreactivity showed a similar distribution pattern in the lumbosacral spinal cord, with the exception that ER-β neurons quite frequently existed in deeper laminae of the dorsal horn. The patterns of location of ER-containing neurons are strikingly similar to the distribution of terminations of visceral primary afferent nerves (in part demonstrated by CGRP immunostaining) in the spinal cord (Cervero and Connell 1984; Roppolo et al. 1985; Kawatani et al. 1990). These ER-positive neurons could be the recipients of sensory information for either reflexes or relays to higher levels. Along this line of thought, Amandusson et al. (1996) have shown that many dorsal horn neurons are ER-α-immunoreactive and contain preproenkephalin mRNA, suggesting that estrogens could regulate enkephalin expression in nociceptive-processing spinal neurons. We have preliminary data that some spinohypothalamic neurons are ER-α immunoreactive. In addition, transmitters in primary afferent nerves, including at least CGRP (Moussaoui et al. 1996) and neurokinins (Duval et al. 1998), can be influenced by estradiol (i.e., in the spinal cord they are downregulated by estradiol). Consequently, if such neurons receive primary afferent input, they may have their activity modulated by estrogens either directly (if they contain ER) or indirectly (if some of their afferent input neurons contain ER). Moreover, since many

ER-β expressing neurons are located in deeper laminae of the dorsal horn, they are in a position to receive afferent inputs from larger-diameter fibers more characteristic of cutaneous or somatic fibers (Cervero and Connell 1984; Roppolo et al. 1985).

In addition, ER-β mRNA-containing neurons were less numerous than the ER-β-immunoreactive cells in the spinal cord of ovariectomized rats. The reason for this differential number is not fully apparent at this time. However, as suggested previously, ER-β might be regulated differently than ER-α and have different functional role(s) from ER-α. Alternative possibilities for fewer ER-β mRNA neurons relative to ER-β-immunoreactive neurons include: (1) that ER-β mRNA has a rapid turnover or is recycled, so ER-β mRNA transcripts are not sufficiently stable to be labeled in high numbers with in situ hybridization, but are translated into ER-β protein, resulting in fewer ER-β mRNA-positive neurons relative to ER-β-immunoreactive neurons; and (2) to get to the level of appropriate detection with the ER-β probe we used a cocktail of two short probes and this may have reduced the sensitivity and thus be expressed with fewer ER-β mRNA cells. Currently it is not known whether one or more of these explanations, or even another, is involved, but it is worth noting that the results of the present in situ hybridization studies with the uterine cervix suggest that the ER-α mRNA transcripts were upregulated in the cervix with loss of estrogen, whereas the ER-β mRNA was not. It is noteworthy that neurons with binding sites for radiolabeled estradiol (Keefer et al. 1973; Morrell et al. 1982) had a distribution similar to the cells containing ER-α and -β that was shown in the present and previous studies (Simerly et al. 1990; Amandusson et al. 1995; Williams and Papka 1996; Shughrue et al. 1997). Taken together, these data confirm that neurons in primary sensory-receptive, sensory relay, and autonomic areas synthesize ER, bind estrogen, and respond to estrogens. Though functional attributes for ER-α are known or are emerging, as of yet, little information is available on the function of ER-β in central or peripheral neurons, though Patrone et al. (2000) suggests that ER-α and ER-β differentially modulate neurites.

In summary, this study using immunohistochemistry and in situ hybridization histochemical techniques has detailed the presence and distribution of ER-α and -β mRNA transcripts and ER-α and -β protein in the female rat lumbosacral spinal cord, L6-S1 dorsal root sensory ganglia, pelvic ganglion, and vagal NG. The distribution of ER-α and -β immunoreactivity in these areas is similar, and this suggests additional circuits and sites of action of estrogen in the nervous system. Uncovering the sites of these two receptors will help to elucidate their function(s) in these areas. Since both isoforms are present in neurons in similar areas, this highlights the possibility of complex control with certain aspects of autonomic and sensory processing.

Acknowledgements We thank Drs. A. Guo and R. Elde (University of Minnesota) for generously sharing their guinea pig antiserum against the capsaicin receptor.

References

Abercrombie M (1946) Estimation of nuclear population from microtome sections. Anat Rec 94:239–247

Adler NT, Davis PG, Komisaruk BR (1977) Variation in the size and sensitivity of a genital sensory field in relation to the estrous cycle in rats. Hormones Behav 9:334–344

Alm P, Lundberg L-M, Wharton J, Polak JM (1988) Effects of pregnancy on the extrinsic innervation of the guinea pig uterus. A histochemical, immunohistochemical and ultrastructural study. Histochem J 20:414–426

Amandusson A, Hermanson O, Blomqvist A (1995) Estrogen receptor-like immunoreactivity in the medullary and spinal dorsal horn of the female rat. Neurosci Lett 196:25–28

Amandusson A, Hermanson O, Blomqvist A (1996) Colocalization of oestrogen receptor immunoreactivity and preproenkephalin mRNA expression to neurons in the superficial laminae of the spinal and medullary dorsal horn of rats. Eur J Neurosci 8:2440–2445

Barde Y-A (1989) Trophic factors and neuronal survival. Neuron 2:1525–1534

Belcher SM (1999) Regulated expression of estrogen receptor α and β mRNA in granule cells during development of the rat cerebellum. Dev Brain Res 115:57–69

Berkley KJ, Robbins A, Sato Y (1988) Afferent fibers supplying the uterus in the rat. J Neurophysiol 59:142–163

Berkley KJ, Hubscher CH, Wall PD (1993a) Neuronal responses to stimulation of the cervix, uterus, colon, and skin in the rat spinal cord. J Neurophysiol 69:545–556

Berkley KJ, Robbins A, Sato Y (1993b) Functional differences between afferent fibers in the hypogastric and pelvic nerves innervating female reproductive organs in the rat. J Neurophysiol 69:533–544

Berman JR, McCarthy MM, Kyprianou N (1998) Effect of estrogen withdrawal on nitric oxide synthase expression and apoptosis in the rat vagina. Urology 51:650–656

Brauer MM, Shockley KP, Chávez R, Richeri A, Cowen T, Crutcher KA (2000) The role of NGF in pregnancy-induced degeneration and regeneration of sympathetic nerves in the guinea pig uterus. J Auton Nerv Syst 79:19–27

Campbell-Thompson ML (1997) Estrogen receptor α and β expression in upper gastrointestinal tract with regulation of trefoil factor family 2 mRNA levels in ovariectomized rats. Biochem Biophys Res Commun 240:478–483

Caterina MJ, Schumacher MA, Tominaga M, RosenTA, Levine JD, Julius D (1997) The capsaicin receptor: a heat-activated ion channel in the pain pathway. Nature 389:816–824

Cervero F, Connell LA (1984) Distribution of somatic and visceral primary afferent fibres within the thoracic spinal cord of the cat. J Comp Neurol 230:88–98

Collins JJ, Lin CE, Berthoud HR, Papka RE (1999) Vagal afferents from the uterus and cervix provide direct connections to the brainstem. Cell Tissue Res 295:43–54

Collins JJ, Wilson K, Fischer-Colbrie R, Papka RE (2000) Distribution and origin of secretoneurin-immunoreactive nerves in the female rat uterus. Neuroscience 95:255–264

Coujard R (1951) Quelques considerations sur le systeme nerveux autonome utero-vaginal. Gynecol Obstet 50:271–296

Couse JF, Korach KS (1998) Exploring the role of sex steroids through studies of receptor deficient mice. J Mol Med 76:497–511

Dufourny L, Warembourg M (1999) Estrogen modulation of neuropeptides: somatostatin, neurotensin and substance P, in the ventrolateral and arcuate nuclei of the female guinea pig. Neurosci Res 33:223–228

Duval P, Lenoir V, Kerdelhue B (1998) Ovarian steroid modulation of neurokinin contents in hypothalamus, pituitary, trigeminal nucleus, and cervical spinal cord of the ovariectomized female rat. J Neuroendocrinol 10:823–828

Friend KE, Resnick EM, Ang LW, Shupnik MA (1997) Specific modulation of estrogen receptor mRNA isoforms in rat pituitary throughout the estrous cycle and in response to steroid hormones. Mol Cell Endocrinol 131:147–55

Furlow JD, Ahrens H, Mueller GC, Gorski J (1990) Antisera to a synthetic peptide recognize native and denatured rat estrogen receptors. Endocrinology 127:1028–32

Gibbs RB, Wu D, Hersh LB, Pfaff DW (1994) Effects of estrogen replacement on the relative levels of choline acetyltransferase, trkA, and nerve growth factor messenger RNAs in the basal forebrain and hippocampal formation of adult rats. Exp Neurol 129:70–80

Gollapudi L, Oblinger MM (1999a) Stable transfection of PC12 cells with estrogen receptor (ERα): protective effects of estrogen on cell survival after serum deprivation. J Neurosci Res 56:99–108

Gollapudi L, Oblinger MM (1999b) Estrogen and NGF synergistically protect terminally differentiated, ERα-transfected PC12 cells from apoptosis. J Neurosci Res 56:471–481

Guo A, Vulchanova L, Wang J, Li X, Elde R (1999) Immunocytochemical localization of the vanilloid receptor 1 (VR1): relationship to neuropeptides, the $P2X_3$ purinoceptor and IB4 binding sites. Eur J Neurosci 11:946–958

Hall JM, McDonnell DP (1999) The estrogen receptor β-isoform (ERβ) of the human estrogen receptor modulates ERα transcriptional activity and is a key regulator of the cellular response to estrogens and antiestrogens. Endocrinology 140: 5566–5578

Hiroi H, Inoue S, Watanabe T, Goto W, Orimo A, Momoeda M, Tsutsumi O, Taketani Y, Muramatsu M (1999) Differential immunolocalization of estrogen receptor α and β in rat ovary and uterus. J Mol Endocrinol 22:37–44

Holzer P (1988) Local effector functions of capsaicin-sensitive sensory nerve endings: involvement of tachykinins, calcitonin gene-related peptide and other neuropeptides. Neuroscience 24:739–768

Honda CN (1985) Visceral and somatic afferent convergence onto neurons near the central canal in the sacral spinal cord of the cat. J Neurophysiol 53:1059–1078

Honjo H, Tamura T, Matsumoto Y, Kawata M, Ogino Y, Tanaka K, Yamamoto T, Ueda S, Okada H (1992) Estrogen as growth factor to central nervous cells – estrogen treatment promotes development of acetylcholinesterase-positive basal forebrain neurons transplanted in the anterior eye chamber. J Steroid Biochem Mol Biol 41:633–635

Houdeau E, Rousseau A, Meusnier C, Prud'homme MJ, Rousseau JP (1998) Sympathetic innervation of the upper and lower regions of the uterus and cervix in the rat have different origins and routes. J Comp Neurol 399:403–412

Kawatani M, Takeshige M, deGroat WC (1990) Central distribution of afferent pathways from the uterus of the cat. J Comp Neurol 320:294–304

Keefer DA, Stumpf WE, Sar M (1973) Estrogen-topographical localization of estrogen-concentrating cells in the rat spinal cord following ^{3}H-estradiol administration. Proc Soc Exp Biol Med 143:414–417

Koike S, Sakai M, Muramatsu M (1987) Molecular cloning and characterization of rat estrogen receptor cDNA. Nucleic Acids Res 15:2499–2513

Komisaruk BR, Adler NT, Hutchison J (1972) Genital sensory field: enlargement by estrogen treatment in female rats. Science 178:1295–1298

Kow L-M, Pfaff DW (1973) Effects of estrogen treatment on the size of receptive field and response threshold of pudendal nerve in the female rat. Neuroendocrinology 13:299–313

Kuiper GG, Enmark E, Pelto-Huikko M, Nilsson S, Gustafsson JA (1996) Cloning of a novel receptor expressed in rat prostate and ovary. Proc Natl Acad Sci USA 93:5925–30

Kuiper GGJM, Carlsson B, Grandien K, Enmark E, Häggblad J, Nilsson S, Gustafsson J-A (1997) Comparison of the ligand binding specificity and transcript tissue distribution of estrogen receptors α and β. Endocrinology 138:863–870

Kuiper GGJM, Shughrue PJ, Merchenthaler I, Gustafsson JA (1998) The estrogen receptor β subtype: a novel mediator of estrogen action in neuroendocrine systems. Front Neuroendocrinol 19:253–286

Kuiper GGJM, Van den Bemd GJCM, Van Leeuwen JPTM (1999) Estrogen receptor and the SERM concept. J Endocrinol Invest 22:594–603

Langub MC Jr, Maley BE, Watson RE Jr (1994) Estrous cycle-associated axosomatic synaptic plasticity upon estrogen receptive neurons in the rat preoptic area. Brain Res 641:303–310

Lee Y, Kawai Y, Shiosaka S, Takami K, Kiyama H, Hillyard CJ, Girgis S, MacIntyre I, Emson PC, Tohyama M (1985) Coexistence of calcitonin gene-related peptide and substance P-like peptide in single cells of the trigeminal ganglion of the rat: immunohistochemical analysis. Brain Res 330:194–196

Li H-Y, Blaustein JD, De Vries GJ, Wade GN (1993) Estrogen-receptor immunoreactivity in hamster brain – preoptic area, hypothalamus and amygdala. Brain Res 631:304–312

Li X, Schwartz PE, Rissman EF (1997) Distribution of estrogen receptor-β-like immunoreactivity in rat forebrain. Neuroendocrinology 66:63–67

Liuzzi FJ, Scoville SA, Bufton SM (1999a) Long-term estrogen replacement coordinately decreases trkA and β-PPT mRNA levels in dorsal root ganglion neurons. Exp Neurol 155:260–267

Liuzzi FJ, Scoville SA, Bufton SM (1999b) Effects of short-term estrogen replacement on trkA mRNA levels in axotomized dorsal root ganglion neurons. Exp Neurol 159:433–440

Lundberg LM, Alm P, Wharton J, Polak JM (1988) Protein gene product 9.5 (PGP 9.5). A new neuronal marker visualizing the whole uterine innervation and pregnancy-induced and developmental changes in the guinea pig. Histochemistry 90:9–17

Matsumoto A, Murakami S, Arai Y (1988) Neurotropic effects of estrogen on the neonatal preoptic area grafted into the adult rat brain. Cell Tissue Res 252:33–37

McEwen B (1996) Gonadal and adrenal steroids regulate neurochemical and structural plasticity of the hippocampus via cellular mechanisms involving NMDA receptors. Cell Mol Neurobiol 16:103–116

McEwen BS, Coirini H, Westlind-Danielsson A, Frankfurt M, Gould E, Schumacher M, Woolley C (1991) Steroid hormones as mediators of neural plasticity. J Steroid Biochem Mol Biol 39:223–232

Mendell LM (1994) Neurotrophic factors and the specification of neural function. Neuroscientist 1:21–29

Miller MM, Hyder SM, Assayag R, Panarella SR, Tousignant P, Franklin KBJ (1999) Estrogen modulates spontaneous alternation and the cholinergic phenotype in the basal forebrain. Neuroscience 91:1143–1153

Morgan C, Nadelhaft I, de Groat WC (1981) The distribution of visceral primary afferents from the pelvic nerve to Lissauer's tract and the spinal gray matter and its relationship to the sacral parasympathetic nucleus. J Comp Neurol 201:415–440

Morrell JI, Wolinsky TD, Krieger MS, Pfaff DW (1982) Autoradiographic identification of estradiol-concentrating cells in the spinal cord of the female rat. Exp Brain Res 45:144–150

Mosselman S, Polman J, Dijkema R (1996) ER beta: identification and characterization of a novel human estrogen receptor. FEBS Lett 392:49–53

Moussaoui S, Duval P, Lenoir V, Garret C, Kerdelhue B (1996) CGRP in the trigeminal nucleus, spinal cord and hypothalamus: effect of gonadal steroids. Neuropeptides 30:546–50

Mufson EJ, Cai WJ, Jafar S, Chen E-Y, Stebbins G, Sendera T, Kordower JH (1999) Estrogen receptor immunoreactivity within subregions of the rat forebrain: neuronal distribution and association with perikarya containing choline acetyltransferase. Brain Res 849:253–274

Murdoch FE, Gorski J (1991) The role of ligand in estrogen receptor regulation of gene expression. Mol Cell Endocrinol 78:103–108

Nahin RL, Madsen AM, Giesler GJ (1983) Anatomical and physiological studies of the gray matter surrounding the spinal cord central canal. J Comp Neurol 220:321–335

Okamura H, Yamamoto K, Hayashi S, Kuroiwa A, Maramatsu M (1992) A polyclonal antibody to the rat oestrogen receptor expressed in *Escherichia coli*: characterization and application to immunohistochemistry. J Endocrinol 135:333–341

Okamura H, Yokosuka M, Hayashi S (1994a) Estrogenic induction of NADPH-diaphorase activity in the preoptic neurons containing estrogen receptor immunoreactivity in the female rat. J Neuroendocrinol 6:597–601

Okamura H, Yokosuka M, McEwen BS, Hayashi S (1994b) Colocalization of NADPH-diaphorase and estrogen receptor immunoreactivity in the rat ventromedial hypothalamic nucleus: stimulatory effects of estrogen on NADPH-diaphorase activity. Endocrinology 135:1705–1708

Osterlund M, Kuiper GG, Gustafsson JA, Hurd YL (1998) Differential distribution and regulation of estrogen receptor-alpha and -beta mRNA within the female rat brain. Brain Res Mol Brain Res 54:175–180

Paech K, Webb P, Kuiper GJM, Nilsson S, Gustafsson J-Å, Kushner PJ, Scanlan TS (1997) Differential ligand activation of estrogen receptors ERα and ERβ at AP1 sites. Science 277:1508–1510

Papka RE, McNeill DL (1992a) Distribution of NADPH-diaphorase-positive nerves in the uterine cervix and neurons in dorsal root and paracervical ganglia of the female rat. Neurosci Lett 147:224–228

Papka RE, McNeill DL (1992b) Coexistence of calcitonin gene-related peptide and galanin immunoreactivity in female rat pelvic and dorsal root ganglia. Peptides 13:761–767

Papka RE, McNeill DL (1993) Light- and electron-microscopic study of synaptic connections in the paracervical ganglia of the female rat: special reference to calcitonin gene-related peptide-, galanin- and tachykinin (substance P and neurokinin A)-immunoreactive nerve fibers and terminals. Cell Tissue Res 271:417–428

Papka RE, Shew RL (1994) Neural input to the uterus and influence on uterine contractility. In: Garfield RE, Tabb T (eds) Control of uterine contractility. CRC Press, Boca Raton, pp 376–399

Papka RE, Traurig HH (1989) Galanin-immunoreactive nerves in the female rat paracervical ganglion and uterine cervix: distribution and reaction to capsaicin. Cell Tissue Res 257:41–51

Papka RE, Traurig HH (1993) Autonomic and visceral sensory innervation of the female reproductive system: special reference to neurochemical markers in nerves and ganglionic connections. In: Maggi CA (ed) Nervous control of the urogenital system. (The autonomic nervous system, vol VI) Harwood Academic, London, pp 421–464

Papka RE, Srinivasan B, Miller KE, Hayashi S (1997) Localization of estrogen receptor protein and estrogen receptor mRNA in peripheral autonomic and sensory neurons. Neuroscience 79:1153–1163

Papka RE, Williams SJ, Miller KE, Copelin TM, Puri P (1998) CNS location of uterine-related neurons revealed by transsynaptic tracing with pseudorabies virus and their relationship with estrogen-receptor-immunoreactive neurons. Neuroscience 84:935–952

Patrone C, Andersson S, Korhonen L, Lindholm D (1999) Estrogen receptor-dependent regulation of sensory neuron survival in developing dorsal root ganglion. Proc Natl Acad Sci USA 96:10905–10910

Patrone C, Pollio G, Vegeto E, Enmark E, Curtis I de, Gustafsson J-Å, Maggi A (2000) Estradiol induces differential neuronal phenotypes by activating estrogen receptor α or β. Endocrinology 141:1839–1845

Paxinos G, Watson C (1997) The rat brain in stereotaxic coordinates, 3rd edn. Academic, New York

Price J (1985) An immunohistochemical and quantitative examination of dorsal root ganglion neuronal subpopulations. J Neurosci 5:2051–2059

Rambourg A, Clermont Y, Beaudet A (1983) Ultrastructural features of six types of neurons in rat dorsal root ganglia. J Neurocytol 12:42–64

Rissman EF, Wersinger SR, Taylor JA, Lubahn DB (1997) Estrogen receptor function as revealed by knockout studies: neuroendocrine and behavioral aspects. Hormones Behav 31:232–243

Robbins A, Berkley K, Sato Y (1992) Estrous cycle variation of afferent fibers supplying reproductive organs in the female rat. Brain Res 596:353–356

Roppolo JR, Nadelhaft I, deGroat WC (1985) The organization of pudendal motoneurons and primary afferent projections in the spinal cord of the rhesus monkey revealed by horseradish peroxidase. J Comp Neurol 234:475–488

Saunders PTK, Millar MR, Williams K, Macpherson S, Harkiss D, Anderson RA, Orr B, Groome NP, Scobie G, Fraser HR (2000) Differential expression of estrogen receptor-alpha and -beta and androgen receptor in the ovaries of marmoset and human. Biol Reprod 63:1098–1105

Schleicher G, Stumpf WE, Thiedemann K-U, Drews U (1985) Autoradiographic binding studies with [^{3}H] oestradiol and [^{3}H] dihydrotestosterone in the autonomic genital ganglion (plexus of Frankenhäuser) of the mouse. Acta Endocrinol 110:572–576

Scoville SA, Bufton SM, Liuzzi FJ (1997) Estrogen regulates neurofilament gene expression in adult female rat dorsal root ganglion neurons. Exp Neurol 146:596–599

Shew RL, Papka RE, McNeill DL (1991) Substance P- and calcitonin gene-related peptide immunoreactivity in nerves of the rat uterus: localization, co-localization and effects on uterine contractility. Peptides 12:593–600

Shughrue PJ, Komm B, Merchenthaler I (1996a) The distribution of estrogen receptor-beta mRNA in the rat hypothalamus. Steroids 61:678–681

Shughrue PJ, Lane MV, Merchenthaler I (1996b) In situ hybridization analysis of the distribution of neurokinin-3 mRNA in the rat central nervous system. J Comp Neurol 372:395–414

Shughrue PJ, Lane MV, Merchenthaler I (1997) Comparative distribution of estrogen receptor-α and -β mRNA in the rat central nervous system. J Comp Neurol 388:507–525

Shughrue PJ, Lane MV, Scrimo PJ, Merchenthaler I (1998a) Comparative distribution of estrogen receptor-α (ER-α) and β (ER-β) mRNA in the rat pituitary, gonad, and reproductive tract. Steroids 63:498–504

Shughrue PJ, Scrimo PJ, Merchenthaler I (1998b) Evidence for the colocalization of estrogen receptor-β mRNA and estrogen receptor-a immunoreactivity in neurons of the rat forebrain. Endocrinology 139:5267–5270

Shughrue PJ, Lane MV, Merchenthaler I (1999) Biologically active estrogen receptor-β: evidence from in vivo autoradiographic studies with estrogen receptor α-knockout mice. Endocrinology 140:2613–2620

Shughrue PJ, Scrimo PJ, Merchenthaler I (2000) Estrogen binding and estrogen receptor characterization (ERα and ERβ) in the cholinergic neurons of the rat basal forebrain. Neuroscience 96:41–49

Simerly R, Chang C, Muramatsu M, Swanson L (1990) Distribution of androgen and estrogen receptor mRNA-containing cells in the rat brain: an in situ hybridization study. J Comp Neurol 294:76–95

Sohrabji F, Miranda RC, Toran-Allerand CD (1994) Estrogen differentially regulates estrogen and nerve growth factor receptor mRNAs in adult sensory neurons. J Neurosci 14:459–471

Sporrong B, Alm P, Owman C, Sjoberg NO, Thorbert G (1981) Pregnancy is associated with extensive adrenergic nerve degeneration in the uterus. An electronmicroscopic study in the guinea-pig. Neuroscience 6:1119–26

Taleghany N, Sarajari S, DonCarlos LL, Gollapudi L, Oblinger MM (1999) Differential expression of estrogen receptor alpha and beta in rat dorsal root ganglion neurons. J Neurosci Res 57:603–615

Thorbert G, Alm P, Owman C, Sjöberg N-O, Sporrong B (1978) Regional changes in structural and functional integrity of myometrial adrenergic nerves in pregnant guinea-pig, and their relationship to the localization of the conceptus. Acta Physiol Scand 103:120–131

Toran-Allerand CD (1976) Sex steroids and the development of newborn mouse hypothalamus and preoptic areas in vitro: implications for sexual differentiation. Brain Res 106:407–412

Traub RJ, Solodkin A, Ruda MA (1989) Calcitonin gene-related peptide immunoreactivity in the cat lumbosacral spinal cord and the effects of multiple dorsal rhizotomies. J Comp Neurol 287:225–237

Traurig HH, Papka RE (1993) Autonomic and visceral sensory innervation of the female reproductive system: special reference to the functional roles of nerves in reproductive organs. In: Maggi CA Nervous control of the urogenital system. (The autonomic nervous system, vol VI) Harwood Academic, London, pp 104–141

Tremblay GB, Tremblay A, Copeland NG, Gilbert DJ, Jenkins NA, Labrie F, Giguere V (1997) Cloning, chromosomal localization, and functional analysis of the murine estrogen receptor beta. Mol Endocrinol 11:353–65

Tuchscherer MM, Seybold VS (1985) Immunohistochemical studies of substance P, cholecystokinin-octapeptide and somatostatin in dorsal root ganglia of the rat. Neuroscience 14:593–605

Villar MJ, Wiesenfeld-Hallin Z, Xu XJ, Theodorsson E, Emson PC, Hökfelt T (1991) Further studies on galanin-, substance P, and CGRP-like immunoreactivities in primary sensory neurons and spinal cord: effects of dorsal rhizotomies and sciatic nerve lesions. Exp Neurol 112:9–39

Williams SJ, Papka RE (1996) Estrogen receptor-immunoreactive neurons are present in the female rat lumbar spinal cord. J Neurosci Res 46:492–501

Willis WD, Leonard RB, Kenshalo DR (1978) Spinothalamic tract neurons in the substantia gelatinosa. Science 202:986–988

Yang YM, Ozawa H, Lu HP, Yuri K, Hayashi S, Nihonyanagi K, Kawata M (1998) Immunocytochemical analysis of sex differences in calcitonin gene-related peptide in the rat dorsal root ganglion, with special reference to estrogen and its receptor. Brain Res 791:35–42

Yuri K, Kawata M (1994) Estrogen affects calcitonin-gene related peptide- and methionine-enkephalin-immunoreactive neuron in the female rat preoptic area. Neurosci Lett 169:5–8

Zoubina EV, Smith PG (2000) Axonal degeneration and regeneration in rat uterus during the estrous cycle. Auton Neurosci Basic Clin 84:176-185